



LUND UNIVERSITY

Imaging of tissue degeneration in knee osteoarthritis using magnetic resonance and synchrotron radiation

Einarsson, Emma

2022

Document Version:

Publisher's PDF, also known as Version of record

[Link to publication](#)

Citation for published version (APA):

Einarsson, E. (2022). *Imaging of tissue degeneration in knee osteoarthritis using magnetic resonance and synchrotron radiation*. [Doctoral Thesis (compilation), Department of Translational Medicine]. Lund University, Faculty of Medicine.

Total number of authors:

1

General rights

Unless other specific re-use rights are stated the following general rights apply:

Copyright and moral rights for the publications made accessible in the public portal are retained by the authors and/or other copyright owners and it is a condition of accessing publications that users recognise and abide by the legal requirements associated with these rights.

- Users may download and print one copy of any publication from the public portal for the purpose of private study or research.
- You may not further distribute the material or use it for any profit-making activity or commercial gain
- You may freely distribute the URL identifying the publication in the public portal

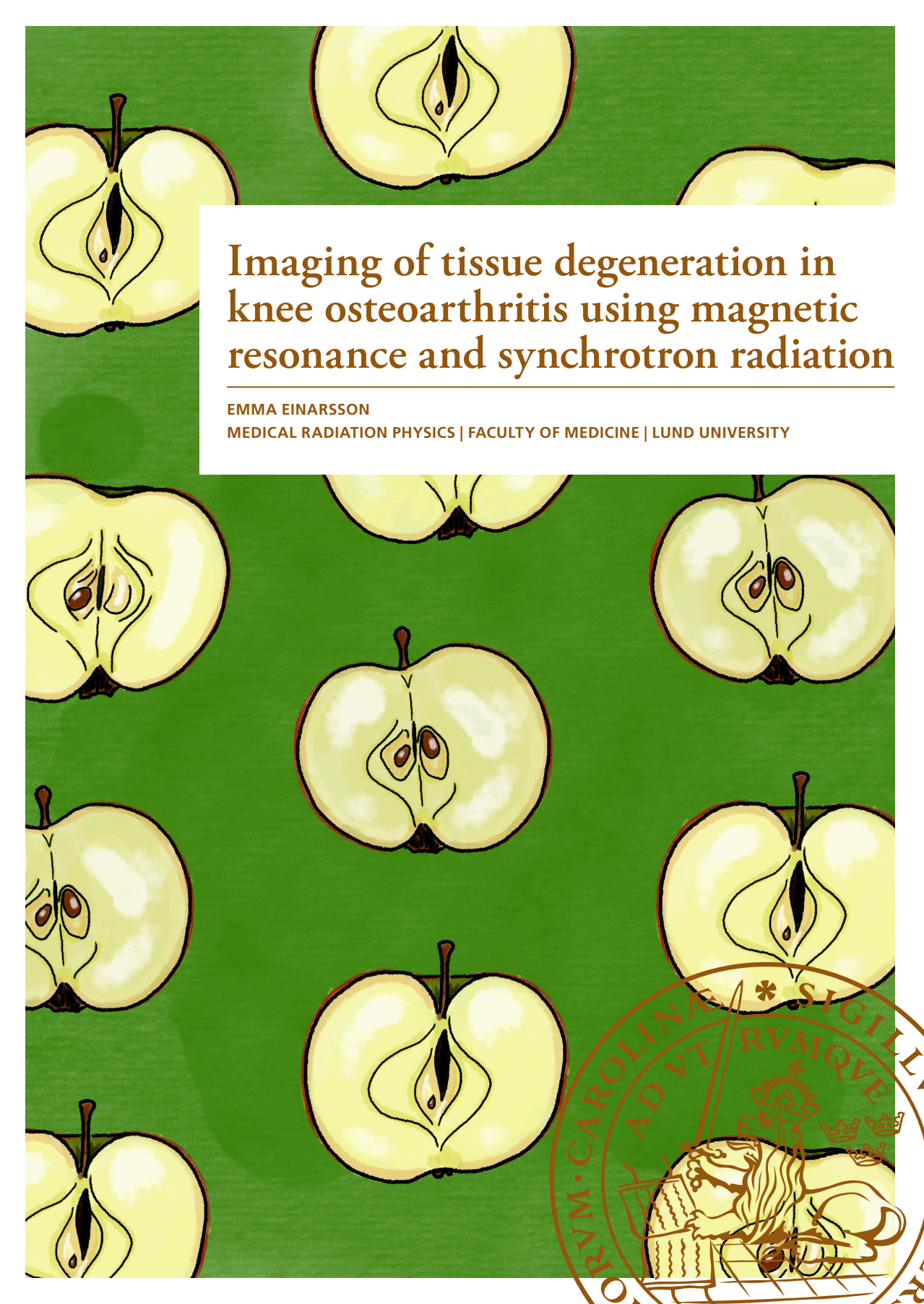
Read more about Creative commons licenses: <https://creativecommons.org/licenses/>

Take down policy

If you believe that this document breaches copyright please contact us providing details, and we will remove access to the work immediately and investigate your claim.

LUND UNIVERSITY

PO Box 117
221 00 Lund
+46 46-222 00 00



Imaging of tissue degeneration in knee osteoarthritis using magnetic resonance and synchrotron radiation

EMMA EINARSSON

MEDICAL RADIATION PHYSICS | FACULTY OF MEDICINE | LUND UNIVERSITY



Imaging of tissue degeneration in knee osteoarthritis using magnetic resonance and synchrotron radiation

Emma Einarsson



LUND
UNIVERSITY

DOCTORAL DISSERTATION

by due permission of the Faculty of Medicine, Lund University, Sweden.
To be defended at Agardhsalen, CRC, Malmö, March 25th at 09:00.

Faculty opponent

Associate Professor Mikko J. Nissi,
University of Eastern Finland, Kuopio, Finland

Organization LUND UNIVERSITY Department of Translational Medicine Medical Radiation Physics, Malmö Author: Emma Einarsson	Document name Doctoral Dissertation Date of issue: 2022-03-25 Sponsoring organization	
Title and subtitle: Imaging of tissue degeneration in knee osteoarthritis using magnetic resonance and synchrotron radiation		
Abstract <p>Osteoarthritis (OA) is a very common disease, especially in the knee. It is characterized by the breakdown of articular cartilage but involves all parts of the joint. OA is usually diagnosed at a late stage when the articular cartilage has begun to disappear. What happens before these macroscopic alterations is to a large extent unknown. In this thesis the focus is on articular cartilage and meniscus and methods to study these tissues.</p> <p>Magnetic resonance imaging (MRI) is suitable for imaging of cartilage and meniscus, and quantitative imaging methods have the potential to probe the molecular composition and microstructure. Using such methods, we can gain new insight in the development of OA and the role of different structures of the knee.</p> <p>The results of this thesis show that MR relaxation times T2*, T2 and T1 are longer in the posterior horn of medial menisci from patients with severe medial compartment knee OA, compared both to the contralateral meniscus and menisci from deceased donors without known knee OA (Paper I). Relaxation times also seem to reflect more subtle changes in the meniscus as they are associated with gold standard histopathological scoring of degeneration characteristics (Paper II).</p> <p>gagCEST is a promising MRI method that has the potential to directly reflect the glycosaminoglycan (GAG) depletion within early degeneration of articular cartilage. However, in a phantom study in this thesis, gagCEST demonstrated a low sensitivity to the type of GAG most abundant in mature human articular cartilage (Paper III).</p> <p>An intrinsic limitation to MRI is the low spatial resolution. Even though MRI-based techniques may have the ability to probe the microscopic composition, other methods are needed to directly visualize the microstructure of the tissue. Here we show that synchrotron radiation (SR)-based microcomputed tomography (μCT) with phase contrast enhancement can resolve the collagen fibre structure of meniscus tissue, including fibre crimping and structural changes related to degeneration (Paper IV). Imaging of tissue samples without fixation or embedding is of interest in studies of meniscus biomechanics.</p> <p>The methods evaluated in this thesis have the potential to detect and follow tissue degeneration in articular cartilage and meniscus and could become valuable tools in future studies to increase our knowledge of disease progression in OA.</p>		
Key words: MRI, osteoarthritis, meniscus, relaxation times, gagCEST, synchrotron radiation-based μCT		
Classification system and/or index terms (if any)		
Supplementary bibliographical information	Language: English	
ISSN and key title: 1652-8220 Lund University, Faculty of Medicine Doctoral Dissertation Series 2022:33		ISBN: 978-91-8021-194-9
Recipient's notes	Number of pages: 59	Price
Security classification		

I, the undersigned, being the copyright owner of the abstract of the above-mentioned dissertation, hereby grant to all reference sources permission to publish and disseminate the abstract of the above-mentioned dissertation.

Signature 

Date 2022-02-17

Imaging of tissue degeneration in knee osteoarthritis using magnetic resonance and synchrotron radiation

Emma Einarsson



LUND
UNIVERSITY

Cover image by E. Einarsson

Copyright pp 1-59 (Emma Einarsson)

Paper 1 © Elsevier Ltd

Paper 2 Open access under Creative Commons (CC-BY) license

Paper 3 © John Wiley & Sons, Ltd

Paper 4 © by the Authors (Manuscript unpublished)

Faculty of Medicine

Department of Medical Radiation Physics

ISBN 978-91-8021-194-9

ISSN 1652-8220

Printed in Sweden by Media-Tryck, Lund University
Lund 2022



Media-Tryck is a Nordic Swan Ecolabel
certified provider of printed material.
Read more about our environmental
work at www.mediatryck.lu.se

MADE IN SWEDEN 

Table of Contents

Abstract	8
Populärvetenskaplig sammanfattning	9
Papers	11
1 Introduction	12
2 Aim	14
3 Cartilaginous structures of the knee.....	15
3.1 Articular cartilage	16
3.2 Meniscus.....	17
4 Imaging-based methods to study tissue degeneration.....	19
4.1 Quantitative MRI.....	20
4.1.1 Relaxation time mapping.....	21
4.1.2 gagCEST.....	24
4.2 SR-based μ CT with phase contrast.....	27
4.2.1 Image analysis	28
5 Tissue samples and phantom construction	30
5.1 Meniscus tissue samples	30
5.2 Proteoglycan phantoms.....	32
6 Results	33
6.1 Relaxation time mapping.....	33
6.2 gagCEST.....	36
6.3 SR-based μ CT with phase contrast.....	37
7 Discussion.....	40
8 Conclusion.....	44
8.1 Relaxation time mapping.....	44
8.2 gagCEST.....	45
8.3 SR-based μ CT with phase contrast.....	45
9 Future work	46
9.1 Relaxation time mapping of human meniscus <i>in vivo</i>	46
9.2 gagCEST in human articular cartilage.....	47
9.3 Meniscus biomechanics	48
10 Acknowledgements.....	49

11	List of abbreviations.....	50
12	References	51

Abstract

Osteoarthritis (OA) is a very common disease, especially in the knee. It is characterized by the breakdown of articular cartilage but involves all parts of the joint. OA is usually diagnosed at a late stage when the articular cartilage has begun to disappear. What happens before these macroscopic alterations is to a large extent unknown. In this thesis the focus is on articular cartilage and meniscus and methods to study these tissues.

Magnetic resonance imaging (MRI) is suitable for imaging of cartilage and meniscus, and quantitative imaging methods have the potential to probe the molecular composition and microstructure. Using such methods, we can gain new insight in the development of OA and the role of different structures of the knee.

The results of this thesis show that MR relaxation times $T2^*$, $T2$ and $T1$ are longer in the posterior horn of medial menisci from patients with severe medial compartment knee OA, compared both to the contralateral meniscus and menisci from deceased donors without known knee OA (**Paper I**). Relaxation times also seem to reflect more subtle changes in the meniscus as they are associated with gold standard histopathological scoring of degeneration characteristics (**Paper II**).

gagCEST is a promising MRI method that has the potential to directly reflect the glycosaminoglycan (GAG) depletion within early degeneration of articular cartilage. However, in a phantom study in this thesis, gagCEST demonstrated a low sensitivity to the type of GAG most abundant in mature human articular cartilage (**Paper III**).

An intrinsic limitation to MRI is the low spatial resolution. Even though MRI-based techniques may have the ability to probe the microscopic composition, other methods are needed to directly visualize the microstructure of the tissue. Here we show that synchrotron radiation (SR)-based microcomputed tomography (μ CT) with phase contrast enhancement can resolve the collagen fibre structure of meniscus tissue, including fibre crimping and structural changes related to degeneration (**Paper IV**). Imaging of tissue samples without fixation or embedding is of interest in studies of meniscus biomechanics.

The methods evaluated in this thesis have the potential to detect and follow tissue degeneration in articular cartilage and meniscus and could become valuable tools in future studies to increase our knowledge of disease progression in OA.

Populärvetenskaplig sammanfattning

Artros är en väldigt vanlig ledsjukdom som ofta drabbar knäleden. Diagnosen ställs ofta först när ledbrusk som klär benytorna i leden börjar försvinna men mer subtila förändringar börjar långt innan dess. Inte bara ledbrusk utan även andra delar av knät är inblandade i utvecklingen av artros, t.ex. menisker, ben och ligament. Den här avhandlingen fokuserar på ledbrusk och menisk och bildbaserade metoder för att studera dessa vävnader och hur de påverkas vid artros.

Glykosaminoglykan (GAG) är en viktig beståndsdel i ledbrusk som drar åt sig vatten medan strikt ordnade fiber bestående av kollagen hindrar vävnaden från att svälla trots den stora mängden vätska. Denna egenskap ger brosket dess viktiga stötdämpande förmåga. I ett tidigt stadium av artros minskar mängden GAG och kollagennätverket börjar brytas ned vilket gör att ledbrusk kan förlora viktiga funktionella egenskaper.

I varje knä finns två menisker som sitter som halvmåneformade kilar mellan lårbenet och skenbenet där de hjälper till att fördela trycket jämnt och avlasta ledbrusk. Vad som händer i menisken vid artros är inte lika väl studerat som i ledbrusk men skador på menisken är vanligt i samband med artros.

Makroskopiska skador på brosk och menisk kan ses med hjälp av magnetkamera (MR). MR är en bildtagningsmetod som inte använder sig av joniserande strålning (som t.ex. röntgen) och som lämpar sig väl för att undersöka leder. MR-bildens egenskaper är beroende av vävnadens struktur och uppbyggnad på en molekylär nivå och olika metoder kan användas för att mäta parametrar som även reflekterar vävnadens egenskaper. Några sådana metoder för användning i ledbrusk och menisk utvärderas i den här avhandlingen.

I två av delarbetena utvärderades mätning av de MR-specifika parametrarna T1, T2 och T2*, även kallade relaxationstider. Dessa parametrar förändras beroende på t.ex. vatteninnehåll och hur strukturerat kollagenet är i brosk och menisk. I utplockade menisker från patienter med långt gången artros visade sig uppmätta relaxationstider vara tydligt längre än i menisker från avlidna donatorer utan någon känd knäledsproblem. Längre relaxationstider var också associerade med högre grad av nedbrytning av vävnaden, utvärderad genom så kallad histopatologi, d.v.s. genom att studera vävnaden i mikroskop. Dessa resultat tyder på att denna typ av

mätningar kan vara användbara metoder för att studera meniskens roll i artrosutveckling.

GAG *chemical exchange saturation transfer* (gagCEST) är en MR-baserad metod som kan detektera förekomsten av GAG i vävnad. Den är därför av stort intresse för att följa förlusten av GAG som sker i ledbrusk vid ett tidigt skede av artros. I försök med GAG i lösning visade våra resultat att det har betydelse vilken sorts GAG man mäter på och att gagCEST-tekniken inte är speciellt känslig för den typ av GAG som dominerar i mänskligt ledbrusk. Detta är ett stort potentiellt problem för metoden och det är därför viktigt med fortsatta studier för att utvärdera om metodens känslighet för olika GAG-typer är densamma i vävnad som i lösning och om gagCEST-tekniken i så fall kan optimeras för att bättre detektera det GAG som finns i ledbrusket.

En begränsning med MR är den låga upplösningen i bilderna. Även om kvantitativa parametrar innehåller information om vävnadens struktur på en mikroskopisk nivå är det också viktigt att kunna observera dessa strukturer mer direkt. Synkrotronljusbaserad mikro-datorotografi (μ CT) med faskontrast är en teknik som kan avbilda vävnadsprover i 3D, utan att förstöra provet, och ger bilder med mycket hög upplösning. Synkrotronljus produceras i en synkrotronljusanläggning där elektroner accelereras till nära ljusets hastighet för att producera röntgenstrålning som bland annat kan användas för bildtagning med μ CT-teknik.

Vid bildtagning med konventionella mikroskopimetoder krävs vanligtvis att vävnaden fixeras i formalin och bäddas in i paraffin vilket är opraktiskt vid studier av vävnadens biomekaniska egenskaper, t.ex. hur den reagerar på tryck. Resultatet i den här avhandlingen visar för första gången att meniskvävnad och dess fiberstrukturer kan avbildas med god upplösning utan fixering eller inbäddning med hjälp av synkrotronljusbaserad μ CT med faskontrast.

Bildtagningsmetoder som de som utvärderats i den här avhandlingen kan bli till stor hjälp i framtida studier som verktyg för att undersöka och följa vävnadens nedbrytning i menisk och ledbrusk i samband med artros.

Papers

This thesis is based on the following papers:

- I. Ultra-high field magnetic resonance imaging parameter mapping in the posterior horn of *ex vivo* human menisci. E. Olsson¹, E. Folkesson, P. Peterson, P. Önnérfjord, J. Tjörnstrand, H.V. Hughes, M. Englund and J. Svensson
Osteoarthritis and Cartilage 27 (2019) 476-483
- II. Relating MR relaxation times of *ex vivo* meniscus to tissue degeneration through comparison with histopathology. E. Einarsson, J. Svensson, E. Folkesson, I. Kestilä, J. Tjörnstrand, P. Peterson, M.A.J. Finnilä, H.V. Hughes, A. Turkiewicz, S. Saarakkala, M. Englund
Osteoarthritis and Cartilage Open 2 (2020) 100061
- III. The role of cartilage glycosaminoglycan structure in gagCEST. E. Einarsson, P. Peterson, P. Önnérfjord, M. Gottschalk, X. Xu, L. Knutsson, L.E. Dahlberg, A. Struglics, J. Svensson
NMR in Biomedicine 2020 May;33(5):e4259
- IV. Phase-contrast enhanced synchrotron micro-tomography of human meniscus tissue. E. Einarsson, M. Pierantoni, V. Novak, J. Svensson, H. Isaksson, M. Englund
Manuscript

¹ E. Einarsson née Olsson

1 Introduction

Pain and reduced joint function are a part of the everyday life for a lot of people who are suffering from osteoarthritis (OA). OA is characterized by the degradation of articular cartilage and can affect almost any joint in the body such as fingers, shoulders, hips, or knees. Of these, OA of the knee is among the most common and often leads to immobility and reduced physical activity. Besides a negative effect on the quality of life due to pain and disability, OA is also associated with a higher risk of cardiovascular disease (Fernandes and Valdes 2015, Wang, Bai et al. 2016, Nelson 2018). OA is very common, and the prevalence is likely to increase as old age and overweight are important risk factors.

Physical activity may prevent development of OA and help relieve mild symptoms, but no cure or disease modifying drug exists. At a late stage, the only option may be to replace the entire knee joint with a prosthesis. A so called total knee joint replacement (TKR) often does not fully restore physical function and, although a knee prosthesis can last for 25 years or longer, it may have to be replaced eventually which is especially important to consider for younger patients (Evans, Walker et al. 2019).

OA is often said to be a wear and tear disease, but its origin and what is happening at early stages remains to be elucidated. Previous meniscus or ligament injury is known to be a risk factor for developing OA. It is thus important to consider the whole joint and not only the articular cartilage when studying the condition (Poole 2012). To be able to follow the disease progression we need methods to detect changes both in macroscopic as well as microscopic structures of the joint tissues.

Evaluation of OA is traditionally made using radiographs. Soft tissue like articular cartilage and menisci are not visible in such images but the space between the bones in the joint can be seen to decrease with progressing OA as the articular cartilage diminishes. Naturally, this method is not sensitive to early degenerative changes and for closer investigation of the different joint tissues it is necessary to study these tissues directly.

Magnetic resonance imaging (MRI) offers high soft tissue contrast, is non-invasive and does not rely on ionizing radiation. It is thus a very suitable method for examination of joint tissues *in vivo*. Although its relatively low spatial resolution, compared to e.g., computed tomography (CT), restricts the use to visualization of macroscopic structures, there exists MRI techniques with the potential of probing

the microstructure and reveal information about the chemical environment in the tissue. Examples of such suggested techniques include sodium (^{23}Na) imaging, glycosaminoglycan chemical exchange saturation transfer (gagCEST) and relaxation time mapping. These kinds of methods are still under development and needs to be validated against gold standard methods before they can be used in e.g. longitudinal studies of OA progression. Especially in the meniscus, work remains to establish which methods can contribute to valuable information about tissue degeneration.

Using *ex vivo* imaging and histology we may also be able to study the tissue microstructure directly and in more detail. Micro computed tomography (μCT) is a 3D imaging method suitable for tissue samples. Synchrotron radiation (SR) and phase contrast can further improve the method with the potential of imaging soft tissue in its native form, i.e. without chemical fixation, embedding or addition of contrast agents. This would be especially beneficial for studies of tissue biomechanics as it could enable imaging during loading.

Development of quantitative and semi-quantitative imaging methods are crucial for further studies that increase our knowledge of this very common and serious disease for the prospect of developing treatment options and/or a cure in the future. In this thesis, methods with the potential to reflect degenerative processes in articular cartilage and meniscus are evaluated.

2 Aim

The aim of this thesis was to investigate the potential of quantitative and semi-quantitative imaging-based methods to evaluate OA-related tissue degeneration and reflect disease severity in meniscus and articular cartilage. More specifically, the aims were

- to investigate if MR relaxation times can be used to discriminate between normal and diseased human meniscus (**Paper I**)
- to relate meniscus relaxation times to degenerative stage as established through gold standard histopathological scoring (**Paper II**)
- to investigate how gagCEST effect relates to GAG concentration for GAG in different forms relevant for articular cartilage (**Paper III**)
- to investigate the feasibility to perform SR-based μ CT with phase contrast enhancement in non-fixed human meniscus tissue (**Paper IV**)

3 Cartilaginous structures of the knee

The knee is one of the joints most commonly affected by OA and all parts of the knee are likely involved in the disease progress (Poole 2012). For example, meniscal damage is associated with development of OA (Englund, Guermazi et al. 2009) and acute injury to ligaments has been seen to be a risk factor (Lohmander, Englund et al. 2007, Barenius, Ponzer et al. 2014, Gong, Pedroia et al. 2016). Also bone deformations and lesions, as well as synovitis, has been reported to be signs of disease in the knee (Baker-LePain and Lane 2012, Felson, Niu et al. 2016). In this thesis, the focus is on articular cartilage and meniscus. This chapter gives a brief overview of the function and structure of these two cartilaginous tissues.

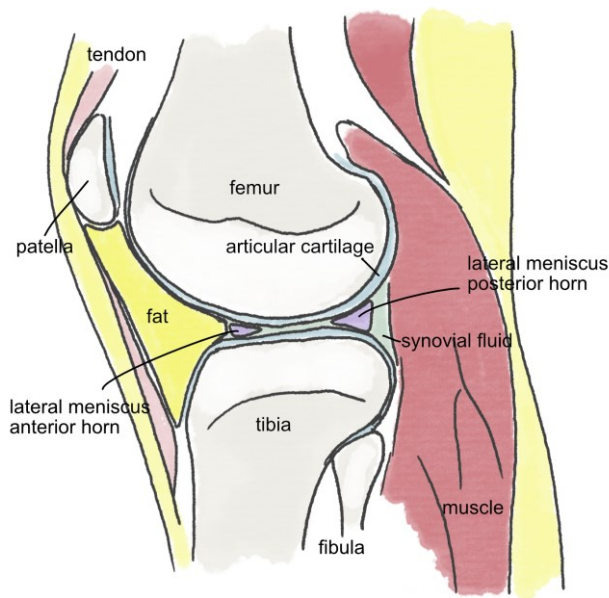


Figure 1 Schematic illustration of a knee in a sagittal plane over the lateral meniscus. The anterior and posterior horn of the meniscus (purple) are seen as triangular shapes between femur and tibia. The bone surfaces of the femoral condyle and the tibial plateau are covered with a layer of articular cartilage (light blue).

3.1 Articular cartilage

The bone surfaces within a joint are covered with articular cartilage (Figure 1) which has the ability to withstand load and reduce friction (Fox, Bedi et al. 2009). Articular cartilage is an avascular tissue with a sparse number of cells and the extracellular matrix consists mainly of water, collagen fibres (collagen type II) and proteoglycans. The collagen fibres are mainly oriented radially at the transition to the bone while more parallel to the surface in the superficial cartilage (Speer and Dahners 1979).

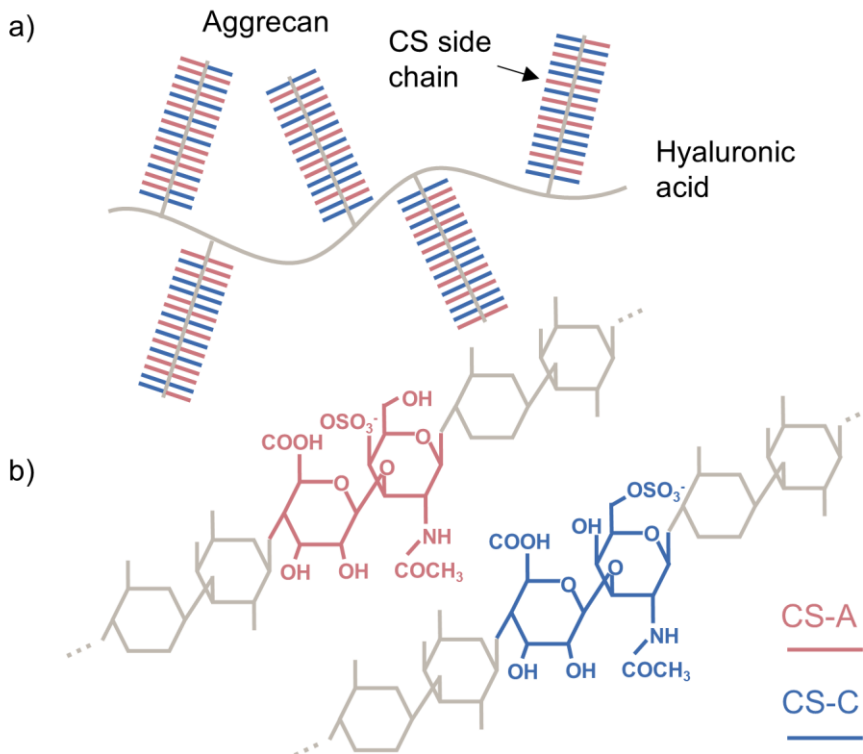


Figure 2 Schematic picture of aggrecan composition with CS-A and CS-C. a) Multiple chains of CS covalently attached to a protein core forms the proteoglycan aggrecan which links to hyaluronic acid. b) chemical structure of CS-A and CS-C, respectively.

Proteoglycans are proteins with covalently attached chains of glycosaminoglycan (GAG). Negatively charged GAG has a key role in the cartilage as it attracts positive sodium ions which in turn leads to an increase in the osmotic pressure. The strict collagen network keeps the tissue from swelling which results in a tissue that can hold a large amount of water and is pressure resistant. Degradation of the collagen

fibres and loss of proteoglycans in the early stages of OA reduces this ability (Martel-Pelletier, Boileau et al. 2008). For studies of OA, methods that are sensitive to disruption of the collagen network and changes in collagen and proteoglycan concentration are thus of interest. In **paper III**, we investigated an MR-based method aiming to estimate GAG content in cartilage tissue.

The most abundant proteoglycan in articular cartilage is aggrecan which has a very large number of GAG chains attached to the protein core (Figure 2a). As the name implies, aggrecan has the ability to form large aggregates which are trapped within the collagen meshwork. This is done by linkage to hyaluronic acid. The most common GAG in aggrecan and cartilage is known as chondroitin sulphate (CS) which exist mainly in the form of type A and C. CS-A and CS-C differ only in the location of the negatively charged sulphate group (Figure 2b) (Pomin 2014). In very young cartilage, the majority of the CS is of type A but with maturation and ageing, type C eventually dominates (Bayliss, Osborne et al. 1999). For the method evaluated in **paper III**, we investigate the importance of distinguishing between these two CS types.

3.2 Meniscus

The medial and lateral menisci are two semi-lunar shaped cartilaginous structures (Figure 3) wedged in between the femur and tibia on each side of the knee joint (Figure 1). The main function of the meniscus is to increase the contact area between the bones to distribute load and reduce the pressure on the articular cartilage (Fox, Wanivenhaus et al. 2015). We studied meniscus tissue using different imaging techniques in **paper I, II and IV**.

Meniscus tissue consists of strictly organized collagen fibres forming thicker bundles that are orientated mainly in a circumferential direction (Petersen and Tillmann 1998). The collagen is of another type (mainly type I) than what is found in articular cartilage and unlike cartilage fibres, the meniscus fibres are crimped, which means they have a wavy shape (Aspden, Yarker et al. 1985, Wren and Carter 1998). In **paper IV**, we can observe this phenomenon directly using a SR-based imaging technique. Crimping of collagen fibres are likely important for the biomechanical properties of the meniscus tissue such as withstanding tensile stress (Diamant, Keller et al. 1972, Michalek, Kuxhaus et al. 2018).

The meniscus is commonly divided into three zones, each constituting a third of the meniscus width from the inner thin tip to the outer border. The outer zone is supplied with blood and nerves while the inner zone is avascular and more similar to articular cartilage as it also contains more collagen type II (Cheung 1987, Folkesson, Turkiewicz et al. 2020).

Damage to the meniscus in form of tears can be acute, e.g. from sport-related injury, or degenerative (Poehling, Ruch et al. 1990). Degenerative tears are common in the middle-aged and elderly population, especially in conjunction with knee OA (Jerosch, Castro et al. 1996, Englund, Guermazi et al. 2008, Englund, Guermazi et al. 2009) and a

torn meniscus may also in some cases be the first sign of incipient OA (Englund, Guermazi et al. 2009). The posterior horn of the medial meniscus has been reported to be especially prone to degeneration (Kumm, Roemer et al. 2016, Dube, Bowes et al. 2018). This is the reason we chose to focus on the posterior horn of patients with medial knee OA in **paper I-II**.

With degeneration, the collagen network gets disrupted. Degenerated menisci have been reported to be larger in size compared to healthy menisci, indicating swelling of the tissue which could be related to the looser collagen structure (Jung, Lee et al. 2010, Kestilä, Folkesson et al. 2019). The increase in water content may be the reason that the concentration of proteoglycan has been reported to decrease in fresh tissue while for dried samples, as seen in histological slices, the proteoglycan content actually increases (Herwig, Egner et al. 1984, Sun, Mauerhan et al. 2012). The measured increase in proteoglycan has been suggested to be a sign of the meniscus ability for regeneration (Adams, Billingham et al. 1983). However, the concentration of proteoglycans in meniscus tissue is much lower compared to articular cartilage (Önnerfjord, Khabut et al. 2012) and imaging methods related to the collagen structure are therefore usually the focus for meniscus research in OA. In **paper II**, we investigated the association of three quantitative MR parameters with meniscus degeneration.

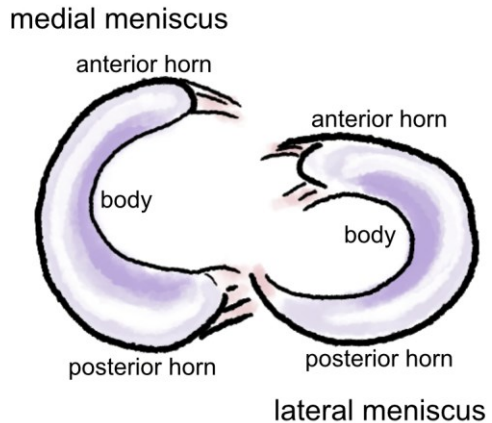


Figure 3 Schematic illustration of the medial and lateral menisci (including meniscal attachments) of a right knee seen from above.

4 Imaging-based methods to study tissue degeneration

MRI is a widely used image modality for examination of joint tissues. It offers non-invasive 3D imaging with good soft tissue contrast and is available at most hospitals. Acquisition parameters can be tailored to achieve images of different desired contrasts, for example as the image in Figure 4. By varying certain parameters in a series of MR measurements and applying appropriate image analysis, MRI can also be used for quantitative measurements of properties that relate to the molecular environment of the tissue. Some quantitative MRI-based methods use standard sequences that are already implemented on clinical systems. Others require special hardware and/or software. Different quantitative MRI-based methods, described in chapter 4.1 below, are evaluated in **paper I-III** for measurements in meniscus and articular cartilage.



Figure 4 Example MRI image of a knee in a sagittal plane centered over the lateral condyle. The image is acquired at 7 T using a 3D SE sequence with fat saturation, 32 ms TE and 1300 ms TR.

An intrinsic limitation of MRI is the low spatial resolution. Histology (Chapter 5.1) and microscopy techniques are useful for visualization of individual structures within the tissue but rely on tissue preparation and staining. An alternative method for non-destructive 3D imaging of *ex vivo* tissue samples is μ CT (Kestilä, Folkesson et al. 2019). Using a SR source and phase contrast enhancement, high resolution can be achieved without the use of chemical fixation and contrast agents (Pierantoni, Silva Barreto et al. 2021). We demonstrate this for meniscus tissue in **paper IV** and the technique is described further in chapter 4.2.

4.1 Quantitative MRI

In MRI, the signal originates from the hydrogen nuclei in the tissue, mainly in water and fat. The hydrogen nuclei have an intrinsic magnetic moment and in a strong magnetic field a net magnetization will arise as they rearrange predominantly in the direction of the external field. This longitudinal magnetization can be manipulated by applying radiofrequency (RF) pulses at a specific frequency (the Larmor frequency) to create a time varying transverse magnetization that can be detected as the MR signal. After RF excitation, the system will return to its equilibrium state through the process known as relaxation. In this process, the MR signal decays (T2 and T2* relaxation) and the initial magnetisation along the main magnetic field is restored (T1 relaxation). The time it takes for the system to relax depends on the molecular composition of the tissue and mapping of relaxation times, conducted through voxel-wise measurements of the time constants T2*, T2 and T1, is therefore of interest in studies of the microscopic conditions of tissue. Except for quantification of relaxation times, also other quantitative imaging methods are available. In this section, a brief overview is given on methods previously used to characterize meniscus and cartilage degeneration. The methods used in this thesis are described more in detail in chapter 4.1.1, 4.1.2 and 4.2.

For research on articular cartilage, most MR-based methods aim to reflect the GAG content or macromolecular structure. Methods like delayed gadolinium enhanced MRI of cartilage (dGEMRIC), gagCEST, ^{23}Na imaging and T1 ρ mapping are all considered to relate to the GAG concentration directly or indirectly while for example T2 mapping, both in articular cartilage and in meniscus, is thought to reflect the integrity of the collagen network (Mosher, Smith et al. 2001, Menezes, Gray et al. 2004). We measure T2 in the meniscus in **paper I-II**, and it is described in more detail below (Chapter 4.1.1.1).

dGEMRIC has until recently been an important method for evaluation of cartilage quality. It has been shown that the cartilage uptake of the ionic Gd-based contrast agent used in this method correlates to the degenerative stage of articular cartilage *in vivo* (Bashir, Gray et al. 1996, Trattnig, Mlynárik et al. 1999). The method is however time consuming and rely on intravenous injection of the contrast agent Gd-DTPA $^{2+}$. Also, due to recent safety concerns regarding the use of such linear Gd-based contrast agents (Gulani, Calamante et al. 2017), dGEMRIC, as it was originally implemented, is no longer an alternative. T1 measurements are the basis of dGEMRIC but is of interest also in native tissue.

T1 ρ is often described as T1 in the rotating frame. It describes the decay of transverse magnetization (Chapter 4.1.1) during a spin-lock pulse. Measurement of T1 ρ requires a non-standard imaging sequence and may be challenging at high field strength due to the high specific absorption rate (SAR) associated with the spin-lock pulse (Singh, Haris et al. 2014).

In ^{23}Na imaging the MR signal comes from sodium instead of hydrogen which is otherwise the standard signal source in MRI. This method is appealing, because the signal intensity in sodium images is, in principle, proportional to the concentration of sodium in cartilage and thus also the concentration of negatively charged GAG (Chapter 3.1). A disadvantage of this method is however the low signal to noise ratio (SNR) due to lower concentration of sodium in the body ($\sim 9 \times 10^{-4}$), and the lower gyromagnetic constant of sodium compared to hydrogen (Brown, Cheng et al. 2014). ^{23}Na imaging also requires special hardware.

Also a few studies have been made exploring the potential of mapping magnetic susceptibility (QSM) in cartilage and meniscus (Wei, Dibb et al. 2017, Wei, Gibbs et al. 2017, Nykänen, Rieppo et al. 2018, Nykänen, Sarin et al. 2019, Wei, Lin et al. 2019, Zhang, Li et al. 2021) and it has been reported that the different layers in cartilage (Chapter 3.1) can be differentiated by the anisotropic susceptibility (Nykänen, Rieppo et al. 2018, Wei, Lin et al. 2019). In meniscus, the measured susceptibility may thus be affected by loss of fibre organisation (Wei, Dibb et al. 2017). QSM in the knee is challenging, compared to for example the brain, due to the structural variety and the presence of fat (Wei, Dibb et al. 2017).

The following sections describe in more detail the methods used in this thesis.

4.1.1 Relaxation time mapping

4.1.1.1 T_2 and T_2^*

In articular cartilage, T_2 and T_2^* have been shown to reflect collagen content and organisation and has been reported to be extended in cartilage affected by OA (Crema, Roemer et al. 2011). In meniscus tissue, T_2 and T_2^* has been reported to increase with degeneration both *ex vivo* and *in vivo* (Williams, Qian et al. 2012, Nebelung, Tingart et al. 2016, Eijgenraam, Bovendeert et al. 2019). In the meniscus, *ex vivo* T_2 has been reported to correlate with water content, surface fraying and cellularity (Son, Goodman et al. 2013, Nebelung, Tingart et al. 2016) while the connection to GAG and collagen content is more uncertain (Son, Goodman et al. 2013).

T_2 and T_2^* relaxation involves dephasing of the transverse magnetisation caused by local field variations originating from the dipole field surrounding each hydrogen nucleus (T_2) and from larger fixed inhomogeneities in the main magnetic field (T_2^*). T_2^* includes both of these effects according to $1/T_2^* = 1/T_2 + 1/T_2'$.

Due to the strict collagen network in articular cartilage, and especially in meniscus (Chapter 3), the movement of water in the tissue is restricted which leads to short T_2 and T_2^* relaxation times. In materials where the hydrogen is more free to move, local field variations are more likely to cancel out, resulting in slower dephasing of the magnetisation.

For healthy knee articular cartilage, T2 has been reported to be about 30-50 ms, varying with cartilage depth and location (Mosher, Smith et al. 2001, Smith, Mosher et al. 2001, Dunn, Lu et al. 2004, Kurkijärvi, Nissi et al. 2004). Meniscus tissue has been reported to have even shorter T2 relaxation times of 8-22 ms (Rauscher, Stahl et al. 2008, Liu, Samsonov et al. 2015, Calixto, Kumar et al. 2016, Hada, Ishijima et al. 2017).

To quantify the relaxation time constant T2 or T2*, a multi-echo sequence is commonly used to capture the signal decay by measurements at different echo times (TE). The signal intensity measured at each TE will then depend on either T2* or T2 according to

$$S \propto S_0 e^{-TE/T2^{(*)}}$$

and the time constant T2^(*) can be estimated by fitting an exponential curve to the measured signal S at different TE (Figure 5).

The signal echoes are generated either only by the normal imaging gradients using a gradient echo sequence (GRE) or by 180° pulses in a spin echo sequence (SE), if we want the measured signal to reflect T2 rather than T2*. The fixed field inhomogeneities (T2') are compensated for by the extra 180° RF pulse at TE/2 that refocus the magnetisation.

TEs should be chosen so that a number of echoes are collected before the signal is lost. For cartilage, and especially meniscus, this may be challenging due to the short T2 in these tissues. To be able to collect the MR signal in the meniscus at several time points before it disappears, an ultrashort echo time (UTE) sequence is preferable (Bae, Du et al. 2010). UTE is a GRE-based sequence specifically adopted to be able to use extremely short TEs. We used an implementation of the UTE sequence in **paper I-II** to obtain multiecho images with a first TE of 0.5 ms for quantification of T2*.

Most tissues have both longer and shorter T2 components and this may be particularly prominent in the meniscus where it can be challenging to achieve short enough TEs. Too long TEs may result in failure to detect short T2 components and hence overestimation of T2 (Kirsch, Kreinest et al. 2013, Juras, Apprich et al. 2014, Liu, Samsonov et al. 2015). The measured value of T2 may thus, to some degree, be dependent on the chosen TEs.

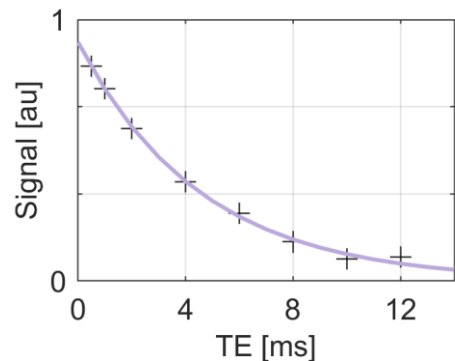


Figure 5 MR signal decay with T2*. Exponential curve fitted to experimental data from an ex vivo medial meniscus imaged at 9.4 T.

Another result of the strict organization of collagen fibres in cartilage and meniscus is that T2 and T2* in these tissues are subject to so called magic angles effects. This means that they are dependent on the orientation of the tissue relative the main magnetic field (Hager, Walzer et al. 2019). They appear the longest at the so-called magic angle at about 54.7° where the dipole field is zero and dipole-dipole interactions are at a minimum. This effect can be seen for example in T2 measurements of femoral cartilage that is curved around the bone. To demonstrate this effect in meniscus, we measured T2* at 7T in an *ex vivo* bovine meniscus in five orientations at different angles to the main magnetic field. When the expected fibre direction of the meniscus was oriented at an angle close to the magic angle, T2* was clearly longer compared to when the meniscus was orientated with its fibres parallel (0°) or perpendicular (90°) to the main magnetic field (Figure 6). To avoid bias from this effect in our measurements of T2 and T2* in human menisci, we did our best to position all samples in the same orientation as would have been the case in an *in vivo* examination (**Paper I-II**).

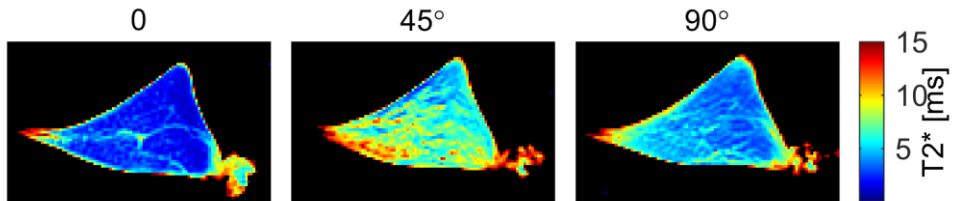


Figure 6 T2* map of bovine meniscus in three different orientations demonstrating the magic angle effect.

4.1.1.2 T1

T1 has not been as extensively studied in cartilage as T2, but has been reported to reflect water content (Berberat, Nissi et al. 2009). T1 has also been reported to be higher in articular cartilage of OA patients compared to healthy subjects although the difference is small (Tiderius, Olsson et al. 2003). In *ex vivo* meniscus, T1 has also been reported to increase with tissue degeneration (Nebelung, Tingart et al. 2016), which we also explored further in **paper I and II**.

The longitudinal relaxation time, T1, describes the relaxation of the magnetization back to the initial state of equilibrium after RF pulses are applied. In contrast to T2 relaxation, this process involves an energy loss as the excitation energy is diffusing through the molecular lattice. The energy transfer is dependent on near-by spins of similar resonance frequency and this likelihood is increased by the presence of paramagnetic elements, e.g. paramagnetic contrast agents, that disturbs the local magnetic field.

In a standard SE experiment, the signal S is dependent on TE and repetition time (TR) according to

$$S \propto S_0 e^{-TE/T_2} (1 - e^{-TR/T_1})$$

T1 can then be estimated by fitting an exponential curve to the signal acquired at different TRs (keeping TE constant) in a similar way as for T2 estimation. We used this method in **paper I-II** as it is fast and implemented as a standard at the scanner that was used in those studies. The gold standard approach, at least at clinical scanners, is otherwise to use inversion recovery (IR) sequences with image acquisition at multiple inversion times (TI). In an IR experiment, the longitudinal magnetization is first flipped 180° before image acquisition at time TI. The signal at this time will be dependent on T1 since different components will have recovered to various extent due to faster or slower T1 relaxation. This method has the advantage of improved SNR but can be time consuming. Other methods available for T1 measurements include variable flip angle (Fram, Herfkens et al. 1987) or a Look-Locker sequence (Look and Locker 1970, Gowland and Mansfield 1993, Kimelman, Vu et al. 2006).

T1 is strongly dependent on field strength. In healthy tissue, T1 has been reported to be about 1000 ms in cartilage at 1.5 T (Tiderius, Olsson et al. 2003) and 1740 ms at 9.4 T (Kurkijärvi, Nissi et al. 2004). In normal meniscus *ex vivo*, T1 has been reported to be about 630 ms at 3 T (Nebelung, Tingart et al. 2016) and we reported values of about 1600 ms at 9.4 T (**Paper I**).

4.1.2 gagCEST

The negatively charged GAGs has a key function in the cartilage (Chapter 3.1) and if we could detect changes in GAG concentration *in vivo* it would most likely be a valuable indicator of the tissue degenerative status. This chapter describes how the CEST technique can be used for detection of GAG.

Hydrogen in metabolites such as GAG, will give rise to an MR signal at a distinct Larmor frequency, different from the frequency of water, but the MR signal from the metabolite would be too weak to image directly. By using the chemical exchange saturation transfer (CEST) technique, such low intensity sources of MR signal can still be detected (Guivel-Scharen, Sinnwell et al. 1998). CEST utilizes that the metabolite pool is connected to the water pool through so called chemical exchange of hydrogen atoms. Because of this exchange, RF saturation at the metabolite frequency will affect the MR signal measured at the water frequency. Since the metabolite pool is refilled with new unsaturated protons from the water pool during RF irradiation the saturation effect will be enhanced by the transfer to water. The decrease in the water signal will be proportional to the concentration of the metabolite.

Saturation can be achieved by applying a train of RF pulses with very high flip angle. The pulsed approach is important to reduce SAR when doing measurements *in vivo*. A too high SAR can otherwise cause increased tissue heating, beyond allowed levels. The design of the saturation pulse train, e.g. B1 power and duty cycle (length of pulses relative to the time in between) is of importance for the measured CEST effect (Saito, Mori et al. 2015, Peterson, Olsson et al. 2019). Saturation is repeated for frequency offsets in a wide range around the water frequency to form a so called CEST (or Z-) spectrum that displays the water signal (S) as a function of saturation frequency (ω), normalized to the unsaturated signal (S_0) (Figure 7).

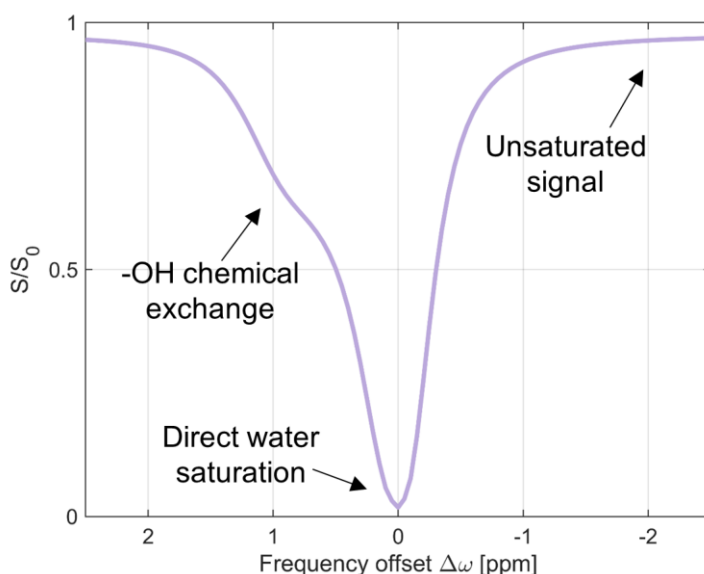


Figure 7 Example of a simulated CEST spectrum with direct water saturation at 0 ppm. Chemical exchange with -OH groups give rise to the small peak at around 1 ppm from water. The unsaturated signal is used for normalization.

The CEST technique has been applied to a lot of different compounds, both naturally occurring in the body and substances that are injected as a form of contrast agents. When targeting the GAG hydroxyl (-OH) groups, we call the method gagCEST (Ling, Regatte et al. 2008). The CEST method specifically targets the metabolite of interest and, in theory, the decrease in the measured signal is proportional to the metabolite concentration. Thus, gagCEST could potentially be used to measure the actual GAG concentration *in vivo*. In **paper III**, we therefore wished to evaluate how gagCEST reflect concentration of GAG relevant for human articular cartilage.

The gagCEST effect is commonly evaluated as the Magnetisation Transfer Ratio asymmetry (MTRasym):

$$MTRasym(\Delta\omega) = \frac{S(\Delta\omega) - S(-\Delta\omega)}{S_0}$$

Where S denotes the water signal at saturation frequency offset $\Delta\omega$ and S_0 denotes the unsaturated signal. MTRasym builds on the assumption that, except for the effect of chemical exchange, the CEST spectrum is symmetric around the water frequency (0 ppm) and by comparing the spectrum at either side of the water peak, the effect of direct water saturation can be subtracted, leaving only the CEST effect. In this way, we calculated an MTRasym spectrum that was averaged over a small interval of 0.7-1.1 ppm to cover the -OH frequency of about 0.9 ppm (**Paper III**).

In practise, the CEST spectrum is not perfectly symmetric and in tissue there can be several sources of CEST effect, with a risk of overlapping peaks. Other ways of evaluating the CEST spectrum exists, for example Lorentzian fitting that has been tested in articular cartilage (Zaiss, Schmitt et al. 2011, Brinkhof, Nizak et al. 2018).

The specific case of gagCEST can be particularly difficult because of the small frequency difference between -OH and water, especially in combination with the wide peaks that are a result of the short T2 of cartilage. Another disadvantage is the fast exchange of the hydrogen between GAG and water, that is close to the limit for CEST to be functional, with the risk of insufficient saturation and further broadening of the -OH peak (van Zijl, Jones et al. 2007). The gagCEST effect can also be influenced by differences in pH (Melkus, Grabau et al. 2014) and in T2 (Müller-Lutz, Schleich et al. 2016). Since T2 may change in connection with degeneration and GAG loss, it is important to consider that there is a potential for bias in the gagCEST effect from changes in T2. The size of both the CEST effect and the potential T2 bias is dependent on the saturation pulse train. A saturation scheme that maximizes the gagCEST effect size is thus not necessarily the one that gives the most information about GAG concentration (Peterson, Olsson et al. 2019).

Because of the stronger magnetization and larger chemical shift, a high field strength is advantageous for the magnitude of the CEST effect (Singh, Haris et al. 2012) which is why we chose to perform our experiments on a 7 T scanner (**Paper III**). However, B0 inhomogeneity is a problem for gagCEST, especially at high field strengths, and leads to uncertainty in the frequency which can result in inaccurate MTRasym values. The Water Saturation Shift Referencing (WASSR) method (Kim, Gillen et al. 2009) is often used to address this issue. Measurements similar to the CEST acquisition are then used but with lower saturation to only affect the water and thus get a more exact measurement of the water frequency in each voxel. This can then be used to shift the CEST spectrum and improve the results.

gagCEST has been implemented for use in both articular cartilage and intervertebral discs. For example, in intervertebral discs, gagCEST measurements has been

compared to morphological scoring as a measure of degeneration (Schleich, Müller-Lutz et al. 2016, Schleich, Müller-Lutz et al. 2016, Wada, Togao et al. 2017, Togao, Hiwatashi et al. 2018) and between healthy and diseased tissue (Haneder, Apprich et al. 2013). In articular cartilage, comparisons have been made with The Visual Analogue Scale (VAS) pain score and different morphological scoring with promising result (Krusche-Mandl, Schmitt et al. 2012, Lee, Yang et al. 2017) and with varying results also to other MR-based methods such as dGEMRIC (Rehnitz, Kupfer et al. 2014), ^{23}Na imaging (Schmitt, Zbýn et al. 2011, Krusche-Mandl, Schmitt et al. 2012), T2 (Krusche-Mandl, Schmitt et al. 2012, Wei, Lambach et al. 2017) and T1 ρ (Kogan, Hargreaves et al. 2017).

Validation of the method has been done mainly with solutions of CS-A which gives an indisputable linear relationship between MTR_{asym} and GAG concentration (Kim, Chan et al. 2011, Wada, Togao et al. 2017). gagCEST effect related to GAG concentration has also been tested indirectly by enzymatic degradation of GAG in animal cartilage (Saar, Zhang et al. 2012). However, while CS-A is the main GAG component in very young cartilage, CS-C is dominating in adult human articular cartilage (Chapter 3.1). It is therefore important that gagCEST is validated also specifically for CS-C (**Paper III**).

4.2 SR-based μCT with phase contrast

The MR-based methods listed above has the potential of probing the microstructure of the cartilage and meniscus tissue and may be important tools to follow and study OA progression in the knee. However, they are all limited by the low spatial resolution of MRI and for certain purposes, e.g. studying the effect of loading on collagen fibres, it may be advantageous to be able to image the fibre structure directly.

Laboratory μCT offers 3D imaging of tissue samples with high resolution that can directly resolve the tissue microstructure. Soft tissue such as meniscus and cartilage attenuate X-rays to a very low degree, traditionally resulting in low contrast. Soft tissue contrast can be achieved by different preparation of tissue such as addition of a contrast agent or drying (Kestilä, Thevenot et al. 2018). Another option is using phase contrast enhancement, a technique where the X-ray beam is allowed to interfere with itself after passing through the sample. This is achieved by moving the detector further away from the sample and results in a diffraction pattern where a difference in refractive index between structures in the tissue sample will lead to a ringing effect that enhances edges in the image (Betz, Wegst et al. 2007).

In a synchrotron facility, electrons are accelerated almost to the speed of light. They are kept rotating in a storage ring using bending magnets that force them into a circular trajectory. When the electrons change path, radiation is emitted in the form of bremsstrahlung. X-rays produced in a synchrotron facility has high flux and high spatial coherence which is ideal for phase contrast imaging. Within the storage ring, additional magnets, in so-called wigglers and undulators, directs the electrons in a wavy path that is customized for production of photons of a desired energy. The photon beam is lead out in a beamline where different experiments can be performed, e.g. tomographic imaging. The TOMCAT beamline at the Swiss Light Source that we used in **paper IV** is such a facility.

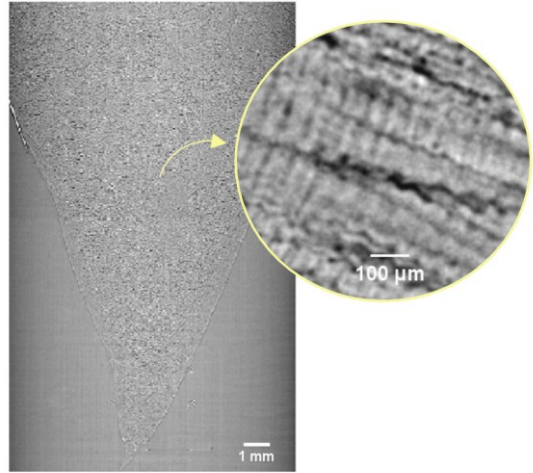


Figure 8 Example of a phase contrast enhanced SR-based μ CT image of a meniscus sample with an enlargement form the central part of the meniscus where crimped collagen fibres can be seen.

Imaging is performed by rotating the sample during irradiation so that projections are collected around the sample. Cross sectional images are then reconstructed, for example using a 3D phase retrieval algorithm such as the Paganin method (Paganin, Mayo et al. 2002). The resulting images will then have a contrast that is dependent both on absorption differences and differences in refractive index (Pierantoni, Silva Barreto et al. 2021). Figure 8 presents a meniscus sample imaged with this technique.

4.2.1 Image analysis

To be able to assess the information in the images and compare tissue appearance in the images to standard measures of tissue degeneration, it would be preferable if image features could be quantified. The quantitative parameters that were used for this purpose in **paper IV** are described in this section.

Orientation analysis using a structure tensor is a method to determine fibre orientation in an image volume originating from material science (Krause, Hausherr et al. 2010). It utilizes a Sobel filter to find gradients in the images and from the gradient images a structure tensor and corresponding eigenvectors are calculated in

each voxel. The third eigenvector of the structure tensor corresponds to the fibre orientation (Mulat, Donias et al. 2008) and can be presented in spherical coordinates as the azimuth and elevation angles describing the direction within the image plane and through the image plane, respectively. Orientation analysis was used to map the azimuth and elevation angle of the collagen fibres in samples of human meniscus imaged using phase contrast enhanced SR-based μ CT in **paper IV**. To only include fibre voxels in the analysis, a mask was calculated based on thresholding of the image intensity. Collagen fibres were assumed to be denser and thus give rise to higher image intensity than the surrounding tissue. The threshold value was set using Otsu's method which minimizes the intensity variation between the two voxel categories, i.e., fibres and background.

To facilitate objective comparison of imaging features between samples, it is preferable to be able to calculate quantitative parameters. In an attempt to quantify the spread in fibre orientation in our meniscus samples we calculated the full area at half maximum (FAHM) from 2D histograms of azimuth and elevation angle maps (Figure 9).

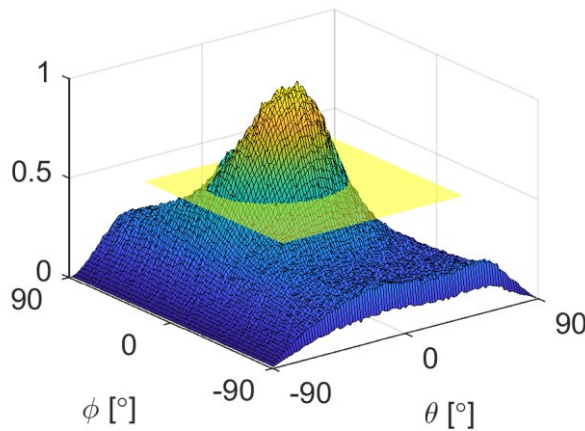


Figure 9 Surface plot of a 2D histogram of azimuth (ϕ) and elevation (θ) angles calculated in fibre voxels within a $0.5 \times 0.5 \times 0.5 \text{ mm}^3$ VOI of a phase contrast enhanced SR-based μ CT image volume of a human meniscus sample. The plane at half of the histogram maximum is marked out in yellow. The area of the histogram in this plane is calculated as the FAHM as a measure of the spread in orientation angles.

The crimping of meniscus collagen fibres is likely related to the biomechanical function of the meniscus tissue and the crimping period could be an interesting parameter to study in relation to meniscus degeneration. The crimping pattern can be clearly seen in phase contrast enhanced SR-based μ CT of meniscus tissue and we made an attempt to measure the crimping period in such images in **paper IV**. The crimping period can be estimated by analysing the frequency components of image profiles drawn along crimped fibres perpendicular to the alternating dark and light bands (Michalek, Kuxhaus et al. 2018).

5 Tissue samples and phantom construction

5.1 Meniscus tissue samples

The meniscus samples that we used in **paper I, II and IV** came from a local biobank at Skane University hospital that includes human samples of meniscus, articular cartilage, blood, and synovial fluid from knee OA patients undergoing TKR surgery or arthroscopy and from deceased donors without known OA. Tissue samples are fresh frozen and stored at -80 °C. For the purpose of **paper I, and II**, lateral and medial menisci were sampled from 10 TKR patients and 10 deceased donors (right knee). Five men and five women were included in each group and the subjects were of a large age span ranging from 18 to 77 years.

Since the posterior horn has been observed to be especially prone to degeneration (Chapter 3.2), this area was of special interest. Thus, from each of the 40 menisci, the posterior horn, including a small part of the body (Figure 10) was cut out for imaging at a 9.4 T preclinical MRI scanner (**Paper I-II**).

For imaging using phase contrast SR- μ CT (**Paper IV**) a 4 mm thick vertical slice was cut from the remaining part of the meniscus body (not the posterior horn), only including menisci from donors without known OA. From 3 of the menisci, an additional slice was cut that was fixed in formalin and sequentially embedded in paraffin (Figure 10)

After MRI, the meniscus posterior horn (and small part of the body) was fixed in formalin and embedded in paraffin, and slices from the imaged volume, were cut out to be evaluated using histopathological scoring. Vertical slices were cut out at two locations: the posterior horn and the body, and horizontal slices were cut out in one location in between (Figure 10). Histology slices were stained with Haematoxylin and Eosin, or Safranin-O Fast Green.

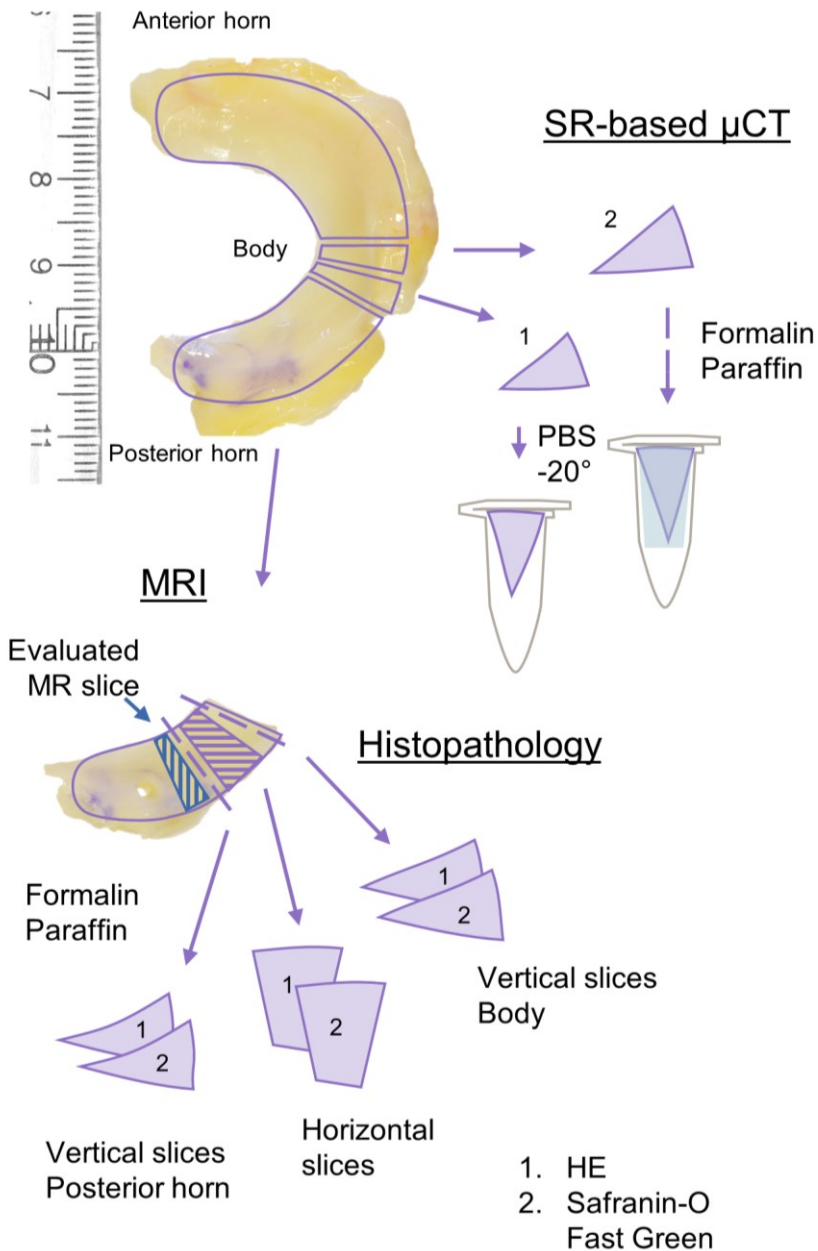


Figure 10 Schematic picture of the dissection of a lateral meniscus for MRI of the posterior horn and SR-based μ CT of samples from the meniscus body, either 1: frozen in PBS or 2: fixed in formalin and embedded in paraffin. The entire posterior horn was imaged using MRI but one slice (its approximate location illustrated in blue) was chosen for further evaluation. For histopathological scoring, vertical and horizontal slices were cut out (after fixation and embedding of the tissue) and stained with 1: Haematoxylin and Eosin or 2: Safranin-O Fast Green.

For the comparison of imaging techniques with histopathological scoring, the vertical histology slices located closest to the volume evaluated by MRI or SR-based μ CT was used in the respective comparison. Collagen organization is most easily evaluated in a horizontal plane, and therefore horizontal slices were cut in one location between the vertical slices. Histopathological scoring of the collagen organization in this location was used for comparison with imaging both in the posterior horn (MRI) and the body (phase contrast SR- μ CT).

Histopathological scoring was performed using Pauli score which evaluates meniscus degeneration based on six categories: Surface integrity at the tibial, femoral and inner border, respectively, collagen organization, cellularity and Safranin O staining intensity (reflecting proteoglycan content). The meniscus is scored 0-3 in each category which is summed up to form the total Pauli score ranging from 0 to 18 where 0 means no degeneration and 18 means severe degeneration (Pauli, Grogan et al. 2011, Kestilä, Folkesson et al. 2019). The histopathological score was considered a gold standard measure of meniscus degeneration and used as a reference when evaluating imaging parameters in relation to degenerative stage in the meniscus in **paper II and IV**.

5.2 Proteoglycan phantoms

For the purpose of evaluating gagCEST dependence on GAG concentration and type in **paper III**, we constructed phantoms with CS-A and CS-C (Chapter 3.1). Powdered CS was dissolved in isotonic solution of PBS in varying concentrations between 0 and 30 mg/ml. PBS was set to about 7.4 by addition of NaOH.

CS can be purchased as a powder labeled either CS-A or CS-C but both will actually be a mixture of different GAGs. Analysis with High Performance Liquid Chromatography (HPLC) fluoroscopy can reveal which disaccharides are present in a mixture, and in what concentrations, (Volpi, Galeotti et al. 2014). We used this technique to determine the concentration of CS-A in our CS phantoms.

To also evaluate solutions with increased molecular complexity, phantoms were prepared with aggrecan in different concentrations. Aggrecan was extracted from calf articular cartilage using guanidine and purified by ultracentrifugation with cesium chloride. The aggrecan was freeze dried so that it could be measured and dissolved in PBS in the same way as for the CS phantoms. Extraction of aggrecan in this way is cumbersome and therefore the amount that could be extracted was enough only for two high concentration phantoms.

6 Results

6.1 Relaxation time mapping

In **paper I**, we mapped relaxation times, T2*, T2 and T1, in the posterior horn of *ex vivo* human menisci at 9.4 T. Example images of a normal and a diseased meniscus are presented in Figure 11e-l. T2*, T2 and T1 in the medial meniscus from deceased donors without known knee OA was (mean and standard deviation) 7.2 ± 2.0 ms, 11.4 ± 3.8 ms and 1590 ± 90 ms respectively. All three relaxation times were significantly longer in medial meniscus from TKR patients with medial compartment knee OA. In lateral menisci, irrespective if they came from donors or patients, relaxation times were similar to the medial donor menisci from knees without known OA (Figure 12).

We also observed, although not statistically significant, a tendency towards longer relaxation times with increasing age among medial donor menisci. If this is in fact a real effect, this suggests that the posterior horn of the medial meniscus could be experiencing degenerative changes related to ageing also in the absence of evident OA.

The histopathological scoring of the menisci presented in **paper II** revealed that also the donor menisci varied in tissue quality with a total Pauli score ranging from 4-16 (including both medial and lateral menisci). The same range of total Pauli score was reported for the menisci from OA patients. There was a clear association between relaxation times and total Pauli score with an increase (95% CI) of 0.62 (0.37, 0.86) ms/score for T2*, 0.83 (0.53, 1.1) ms/score for T2 and 24.7 (16.5, 32.8) ms/score for T1 (Figure 13).

In **paper II**, comparisons of meniscus relaxation times were also made to the Pauli score of specific categories (Chapter 5.1). In general, 95% CIs of the mean difference in T2*, T2 and T1 between menisci of different Pauli score were broad although systematically skewed towards an increase in relaxation times with increasing Pauli score in all categories.

No clear variation was seen in relaxation times with the distance from the inner border, i.e., between meniscus zones (Chapter 3.2). If anything, relaxation times were shorter in the middle zone compared to both the inner and outer zone.

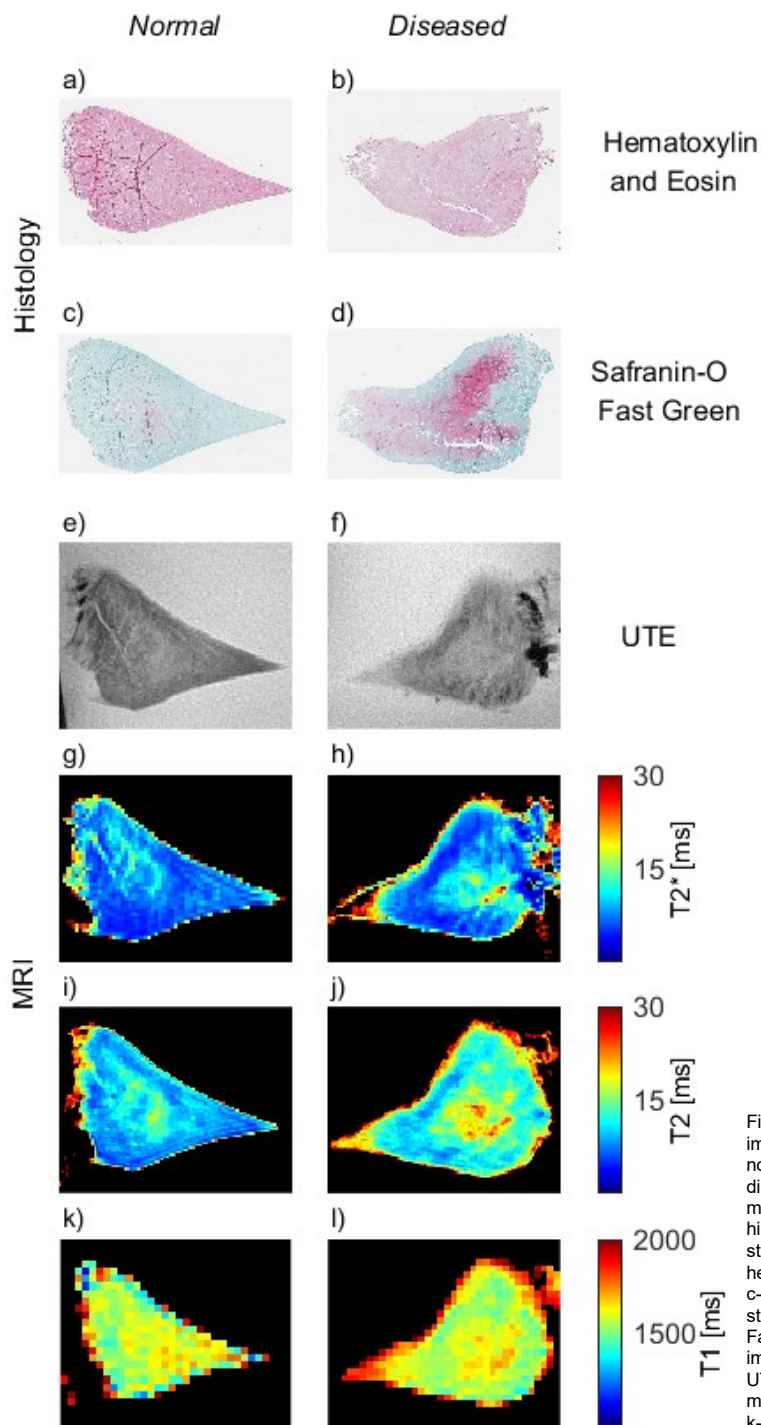


Figure 11 Example images of a lateral normal meniscus and a diseased medial meniscus. a-b) histological slices stained with hematoxylin and eosin, c-d) histological slices stained with Safranin-O Fast Green, e-f) MRI images acquired with an UTE sequence, g-h) T2* maps, i-j) T2 maps and k-l) T1 maps.

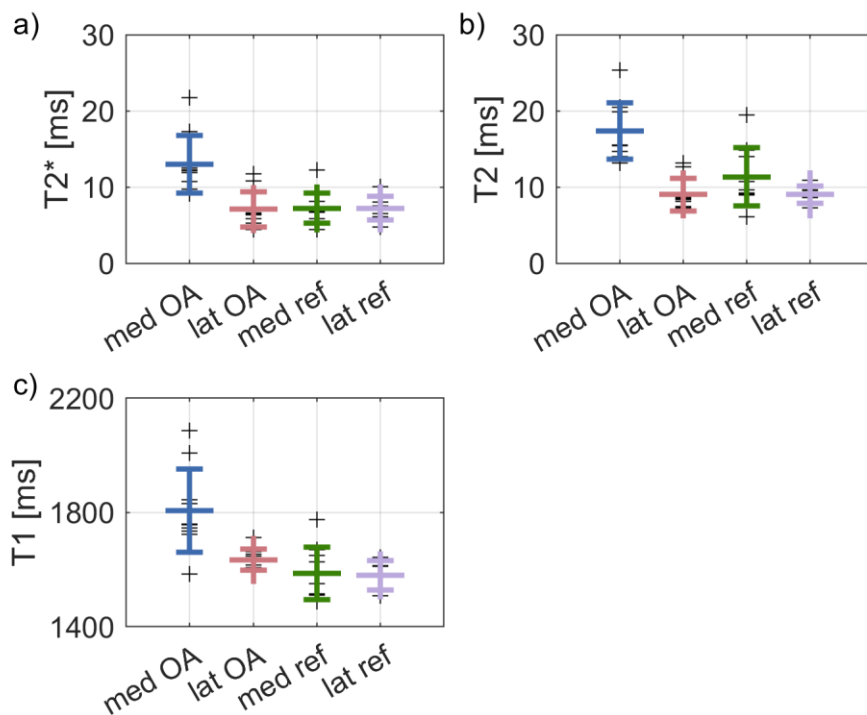


Figure 12 T2*, T2 and T1 in the posterior horn of medial and lateral menisci from OA patients and deceased donors. The larger markers in colour represents mean value and standard deviation within each group.

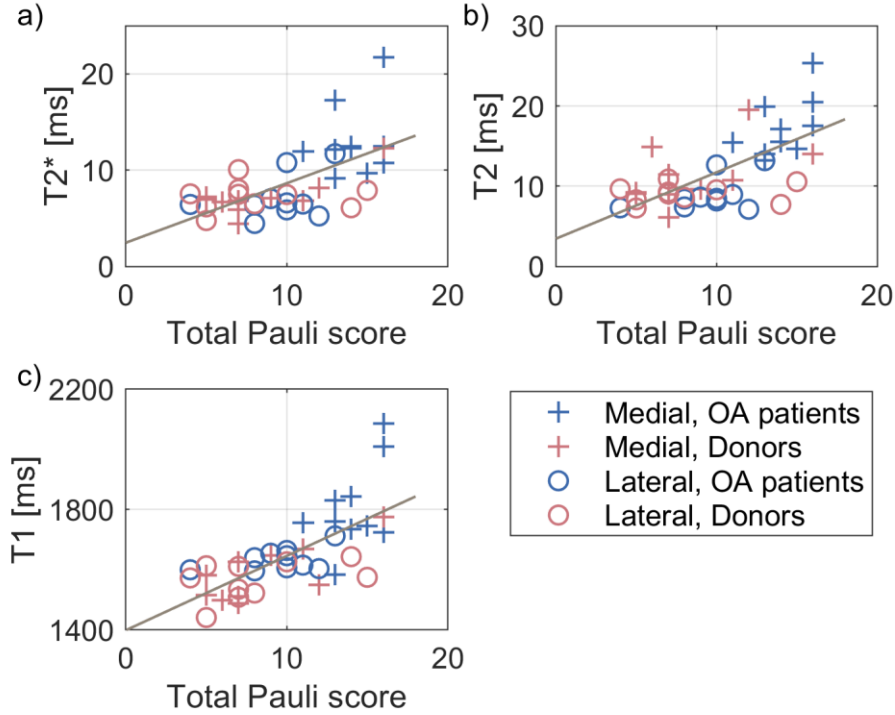


Figure 13 MR relaxation times T2* (a), T2 (b) and T1 (c) presented as a function of total Pauli score as a measure of tissue quality. Lines are representing mixed effect linear regression for all menisci. The slope is statistically significant in all three cases.

6.2 gagCEST

In **paper III**, we saw that the gagCEST effect as evaluated by MTR_{asym} was clearly associated with GAG concentration and the relationship seemed to be linear (Figure 14). However, the size of the effect was dependent on the type of GAG. Our results indicated that, in a mixture of CS-A and CS-C, the effect from CS-C (if existing) is negligible compared to the clear effect originating from CS-A (Figure 14). Phantoms with GAG bound in aggrecan, extracted from young bovine cartilage, gave a similar gagCEST effect as the phantoms containing mainly CS-A (Figure 14a) indicating that the GAG bound in aggrecan is not a problem for gagCEST.

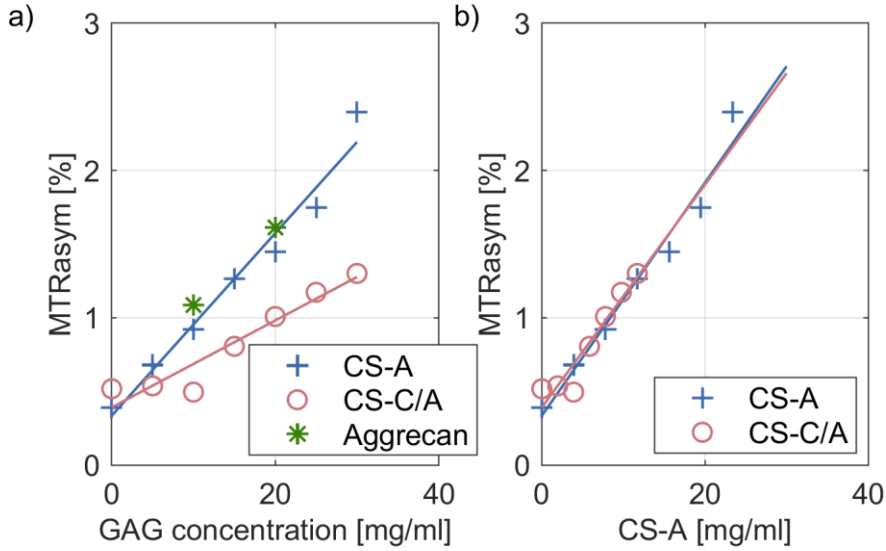


Figure 14 MTRasym, as a measure of gagCEST effect, presented as a function of a) total GAG concentration (a mixture of CS-C and CS-A) and b) concentration of CS-A specifically, for the two phantom series CS-A (78% CS-A, 15% CS-C) and CS-C/A (39% CS-A, 34% CS-C). Also, the two phantoms containing aggrecan (assumed to consist of mainly CS-A but exact concentration is unknown) are included in a). The lines that represent linear regression are aligned when only CS-A is considered as the source of gagCEST effect.

6.3 SR-based μ CT with phase contrast

Imaging of meniscus tissue samples using SR-based μ CT with phase contrast enhancement (**Paper IV**) resulted in high resolution images where the collagen fibre structure and crimping patterns were clearly visualized. Fixed and paraffin embedded samples appeared smoother and with higher contrast between fibres and surrounding tissue compared to the samples that was imaged thawed in PBS. The mean spatial resolution, however, was similar in the images: 5.55 μ m for the paraffin embedded sample and 5.45 μ m in the sample frozen in PBS. Overall, the image quality was satisfactory and did not substantially differ between the different preparation schemes.

Images from degenerated meniscus samples were visually different compared to normal tissue. In general, the collagen network appeared less strict, with less visible crimping and larger cavities in the degenerated samples (Figure 15).

As expected, collagen fibres were seen to be oriented mainly in a circumferential direction in the meniscus. In the example orientation maps in Figure 16, this corresponds to the horizontal direction which is reflected by azimuth and elevation angles close to 0, i.e., turquoise in this colour scale.

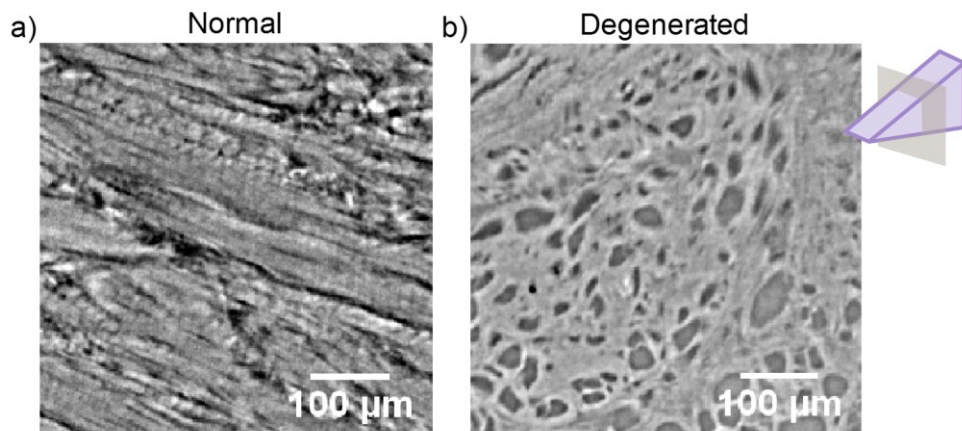


Figure 15 Example images in a sagittal plane of the meniscus, as indicated by the schematic picture, of two samples from the same meniscus, prepared with different preparation schemes: a) fixed in formalin and embedded in paraffin, b) frozen fresh in PBS and thawed before imaging. Crimped collagen fibres can be clearly seen in both samples.

The FAHM of azimuth and elevation angle histograms was calculated as a potential measure of spread in fibre orientation and was expected to increase with collagen fibre disorganization. However, no clear association could be seen with tissue degeneration evaluated by histopathological scoring.

The crimping pattern of collagen fibres can be seen in the images as alternating bright and dark bands perpendicular to the fibre direction (see for example the image in Figure 15a). The mean crimping period was measured to $23.8 \pm 3.1 \mu\text{m}$ but no clear association of crimping period with degeneration could be seen.

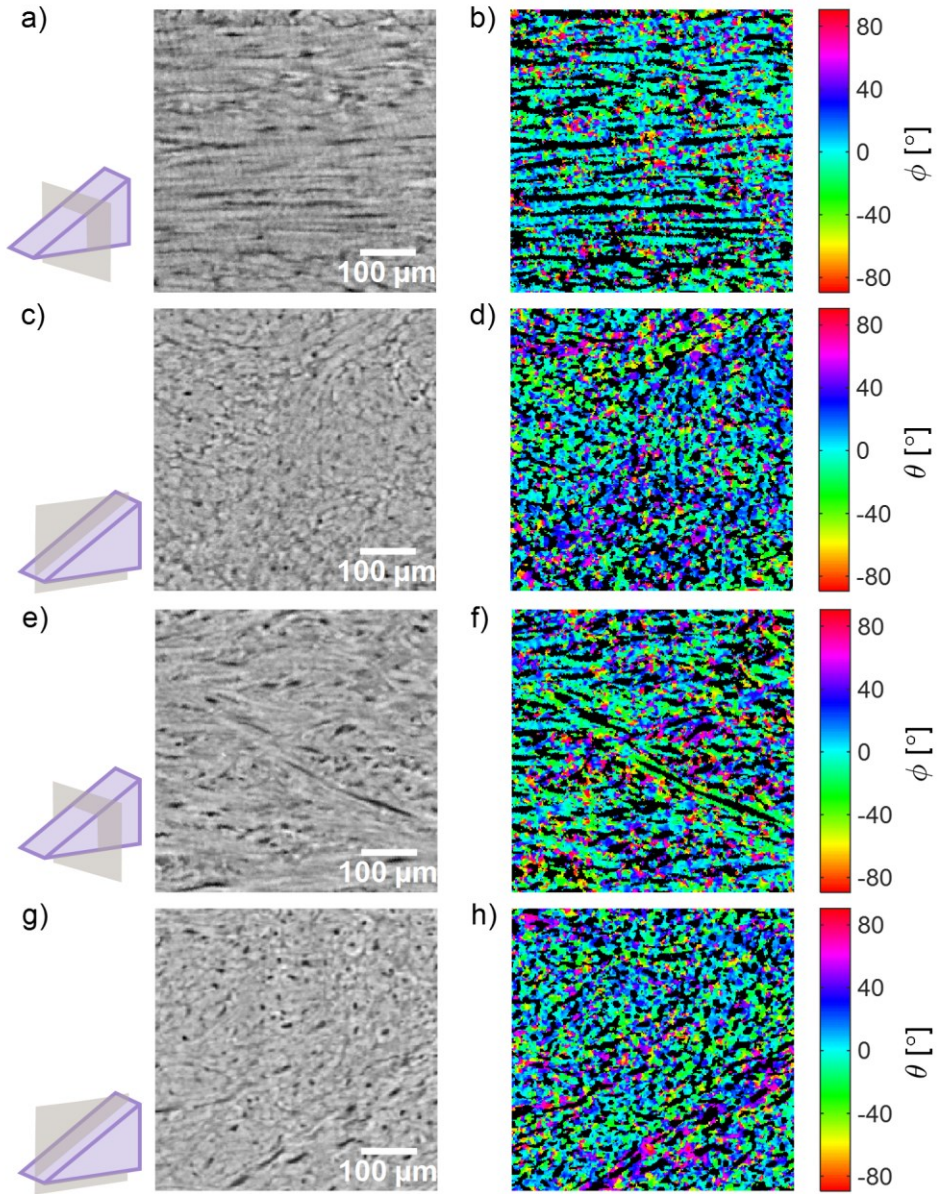


Figure 16 Example images from a small ($0.5 \times 0.5 \times 0.5 \text{ mm}^3$) VOI evaluated with the orientation analysis in the middle (a-d) and inner zone (e-h) of a normal meniscus. a) and e) presents images in the sagittal plane, i.e., parallel to the main direction of the fibres, which is seen as turquoise in the corresponding azimuth (ϕ) maps (b and f). c) and d) presents images in the coronal plane, i.e., perpendicular to the main direction of the fibres, which is also seen as turquoise in the corresponding elevation (θ) angle orientation maps.

7 Discussion

In this thesis, we have evaluated different image-based methods that could potentially be used for quantification of meniscus and cartilage degeneration associated with knee OA.

Mapping of relaxation times, histopathological scoring and SR-based μ CT were all conducted on the same meniscus samples. A strength with this material is that it includes both normal tissue from deceased donors without known OA and samples from OA patients as well as medial and lateral menisci from all subjects which enables paired comparisons.

We report that T2, T2*, and T1 are longer in menisci from diseased compared to normal knee compartments (**Paper I**). This is in agreement with previous publications reporting MR relaxation times in meniscus (Williams, Qian et al. 2012, Nebelung, Tingart et al. 2016). In **paper II**, we compared relaxation times to Pauli scores of individual categories and found that all three relaxation times seemed to be associated with surface integrity and collagen organization. Nebelung et al. also reported that MR relaxation times correlated with histopathological scoring of surface and matrix integrity and of cellularity, using a variant of the Pauli score. In our study, only T1 showed a significant association with cellularity. However, relaxation times seemed to generally increase with scores in all categories in the Pauli scoring system and the categories are likely to be associated with each other since they all describe features related to degeneration.

Due to the difference in structure between the inner and outer zones of the meniscus, we expected relaxation times to vary between the zones, but similar to the results of Williams et al. and Nebelung et al., we did not see a clear difference. There might, however, exist a tendency towards shorter relaxation times in the middle zone compared to the other zones. If so, this may be explained by an increase in relaxation times due to a leakage of surrounding PBS into the tissue. Since the surrounding is different for a meniscus in a knee, it is important that further *in vivo* studies are conducted to confirm our *ex vivo* results. In a study by Eijgenram et al. (Eijgenraam, Bovendeert et al. 2019), T2 was measured *in vivo* in meniscus of TKR patients before surgery. The results of that study suggests that at least T2 reflects degeneration also *in vivo* which is promising as such measurements could then be used as a marker in future longitudinal studies of the meniscus role in OA progression.

There are advantages of doing *ex vivo* and *in vitro* imaging, especially for validation since biochemical and histological methods can be used to establish a ground truth. For example, we used histopathological grading of our meniscus samples to determine degenerative status as a basis for comparison of MR relaxation times. When constructing a phantom, chemical composition and concentrations as well as pH can be controlled in a way that cannot be done *in vivo*, such as in our investigation of gagCEST dependence on GAG concentration in **paper III**. However, it is difficult to know how the conditions change compared to *in vivo* and how it affects the outcome of the experiment. Hence, effects detected *ex vivo* or *in vitro*, has to be confirmed through appropriate *in vivo* measurements.

gagCEST has been implemented as a method to determine tissue quality in articular cartilage e.g., of the knee and wrist (Schmitt, Zbýn et al. 2011, Krusche-Mandl, Schmitt et al. 2012, Singh, Haris et al. 2012, Rehnitz, Kupfer et al. 2014, Schreiner, Zbýn et al. 2016, Kogan, Hargreaves et al. 2017, Krishnamoorthy, Nanga et al. 2017, Lee, Yang et al. 2017, Wei, Lambach et al. 2017, Brinkhof, Nizak et al. 2021). Attempts to relate the gagCEST effect to GAG concentration has commonly been made using phantoms with CS-A. However, the main GAG component in adult human articular cartilage is CS-C (Bayliss, Osborne et al. 1999) and we could demonstrate that in phantoms including a mixture of the two CS types, little or no CEST effect is originating from CS-C (**Paper III**). Thus, in phantoms, gagCEST fails to detect the type of GAG that is most relevant for studies of OA.

We did not expect the small difference in molecular structure between CS-A and CS-C (Chapter 3.1) to have such a big influence on the gagCEST effect and following these unexpected results, an important question is of course how well the phantoms represent the conditions in human tissue. Aiming to relate gagCEST measurements to biochemically determined GAG concentrations in human articular cartilage, we designed an *ex vivo* experiment using human hip articular cartilage collected from patients

undergoing hip replacement due to fracture. Areas of visually intact cartilage was marked out on the surface of 7 femoral heads and imaged while submerged in PBS using our gagCEST protocol as described in **paper III**. After MRI, the cartilage in the imaged areas were cut from the bone so that aggrecan could be extracted and the GAG content determined using Alcian blue precipitation (Björnsson 1993).

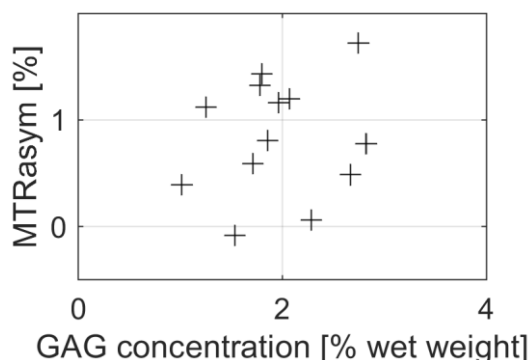


Figure 17 MTRasym measured in *ex vivo* hip cartilage compared to GAG concentration determined using Alcian blue precipitation of the cartilage samples after imaging.

MTRasym values in these measurements did not appear to be associated with GAG concentration (Figure 17). One hypothesis to explain this result could be that the GAG content in the cartilage from these elderly hip replacement patients would be predominantly CS-C. Then, if gagCEST is not sensitive to CS-C, as suggested by the result in **paper III**, it could explain why these measurements resulted mainly in noise. However, it cannot be entirely ruled out that other difficulties, e.g. that the cartilage was very thin and that T2 is much shorter in cartilage compared to phantoms, could have influenced the result. Either way, it is a good example showing how challenging it can be to implement gagCEST in actual cartilage. In a recent paper by Brinkhof et al. (Brinkhof, Nizak et al. 2021), *in vivo* measurements of gagCEST in articular cartilage in patients before TKR surgery was compared to biochemically determined GAG content and the association was found to be moderate at best. Similar results has been reported for comparison of gagCEST to dGEMRIC (Rehnitz, Kupfer et al. 2014) In both studies, gagCEST still seemed to reflect cartilage quality.

The MR based methods discussed so far are developed with the aim to be able to assess tissue quality *in vivo*. To be able to directly visualize the microstructure of the tissue, however, we are relying on *ex vivo* imaging methods, and it is preferable if these methods can be applied on tissue as close to its native form as possible to still be relevant for the tissue *in vivo*.

Phase contrast enhanced SR-based μ CT is an interesting experimental method that could potentially be used to further increase the knowledge of the microscopic structure and function of meniscus tissue. This is, to the best of our knowledge, the first time this method has been used with the purpose to investigate the microstructure of the meniscus. The advantage of this technique over other microscopy methods is that it is a non-destructive 3D imaging technique and that it may be used on non-fixated tissue, as we illustrate in **paper IV**. Especially interesting was the possibility to visualize collagen crimping in the meniscus. Although this is not new in the literature (Aspden, Yarker et al. 1985), it is our perception that this is not common knowledge among OA researchers.

The possibility of imaging non-fixed tissue is of great interest for future studies of meniscus biomechanics as it enables studies of the microstructure under different loading conditions. To evaluate the images, quantitative measures reflecting degenerative changes are needed. We suggested to use FAHM of 2D histograms as a measure of the spread in fibre orientation angles to include both the elevation angle and the azimuth angle. We did not see a clear association with histopathological scoring which suggests the FAHM might not be a sensitive measure of tissue degeneration. However, the horizontal histology slices that was used for evaluation of collagen organisation were cut from the posterior horn and not from the body of the meniscus where the samples were taken for SR-based μ CT imaging (Chapter 5.1). Since meniscus degeneration is often seen to start in the posterior horn, the state of the collagen network might differ between these two locations. Also, the

sample size was limited in this initial study, and it is therefore warranted to further explore the potential usefulness of this parameter.

The crimping pattern of meniscus collagen fibres has been investigated in a few studies using other microscopy imaging techniques. For example, Michalek et al. (Michalek, Kuxhaus et al. 2018) measured crimping frequency in deer menisci to evaluate meniscus swelling related to proteoglycan content. We used the same method to determine crimping period in **paper IV** and found the crimping period of our samples to be similar to the normal deer menisci. Values of about the same order of magnitude were also reported by Villegas et al. (Villegas and Donahue 2010) who measured the crimping in human meniscal attachments.

We did not see an association of crimping period with meniscus degeneration but as the image profiles investigated in this study were drawn manually and at arbitrary locations in the menisci, the uncertainty in the measured values of the crimping period was probably large. There is also a possibility that degeneration is not actually reflected in the crimping period of the unloaded meniscus and that it may be a more interesting parameter to investigate in an experiment of the biomechanical function.

Our meniscus measurements included samples from 10 donors and 10 OA patients. This limited sample size, although enough to show differences in relaxation times between the groups, might have added difficulty to observe more subtle differences and associations, for example variations with Pauli scores in specific categories. Even fewer samples were used in **paper IV** due to limitations in beam time and restriction in access to the synchrotron facility. A larger sample size could aid in getting more conclusive results.

Another limitation is that the tissue samples were frozen. This choice was made for practical reasons, but the freezing process might have altered the tissue structure, e.g., by disruption of collagen fibres and cells (Gelber, Gonzalez et al. 2008).

The purpose of evaluating the MR-based methods was that they could hopefully be used *in vivo* in longitudinal studies. The feasibility of *in vivo* imaging using these methods remains to be evaluated in future work.

8 Conclusion

In general, the work presented in this thesis shows that imaging methods have the potential to reveal structural and molecular changes of cartilaginous tissues related to degenerative processes in knee OA, both through direct visualization using the SR-based μ CT (**Paper IV**), and indirectly by measuring quantitative parameters (**Papers I-II**). Further, this thesis illustrates the importance of studying the biochemical prerequisites of quantitative imaging techniques before implementation *in vivo* (**Paper III**).

Quantitative MRI has the ability to probe the microstructure and reflect changes on a molecular level. For example, we report that MR relaxation times reflect meniscus tissue degeneration. However, the results we have seen in our *ex vivo* (**Paper I-II**) and *in vitro* (**Paper III**) MRI studies remains to be confirmed also *in vivo*. Phase contrast enhanced SR-based μ CT is a promising technique for future studies of meniscus microstructure and biomechanics (**Paper IV**), but further work is needed to establish reliable and useful quantitative measures.

The conclusions of this thesis are listed more specifically for each method below.

8.1 Relaxation time mapping

In **paper I and II**, we report that relaxation times T1, T2 and T2* generally increases with the degree of degeneration as assessed through gold standard histopathology in *ex vivo* human menisci and are longer in the medial meniscus from medial compartment end stage knee OA patients compared both to the lateral meniscus of the same knee and to menisci from donors without known OA.

8.2 gagCEST

The sensitivity of gagCEST vary between different types of GAGs. Even the small difference in chemical structure between type A and C of CS appeared to be crucial for the measured gagCEST effect. We discovered that in phantoms with a mixture of the two, no or little effect originates from CS-C, i.e., the dominating type of GAG in mature human articular cartilage (**Paper III**).

8.3 SR-based μ CT with phase contrast

SR-based μ CT with phase contrast is feasible in human meniscus samples without the use of tissue fixation or embedding, resulting in high resolution images where collagen structure, including crimping, can be clearly visualized (**Paper IV**).

9 Future work

9.1 Relaxation time mapping of human meniscus *in vivo*

Mapping of MR relaxation times are promising methods to noninvasively follow meniscus degeneration as T2*, T2 and T1 seems to reflect tissue degeneration *ex vivo*. However, quantitative parameters may also be influenced by circumstances other than the intended and it is therefore of great importance that estimation of relaxation times as markers for meniscus degeneration is further evaluated also *in vivo*.

We have started up an *in vivo* study including healthy volunteers and OA patients, undergoing knee MRI at 7T. The imaging protocol includes morphological sequences and sequences for quantitative evaluation, such as a multi-TE UTE sequence for mapping of T2* in the meniscus, and a multi-TE SE sequence mainly intended for evaluating T2 in the femoral articular cartilage. For the meniscus, we chose to focus on T2* because of the difficulty to reach short enough TEs in the meniscus using SE-based sequences. This data set will enable *in vivo* confirmation of our *ex vivo* results, regarding the usefulness of relaxation times as a measure of tissue degeneration in OA. If these results prove to be as promising as our *ex vivo* results, relaxation times may be important tools for future longitudinal investigations of the meniscus role in OA.

Figure 18 presents an example MR image in the knee of a healthy volunteer and corresponding T2* map.

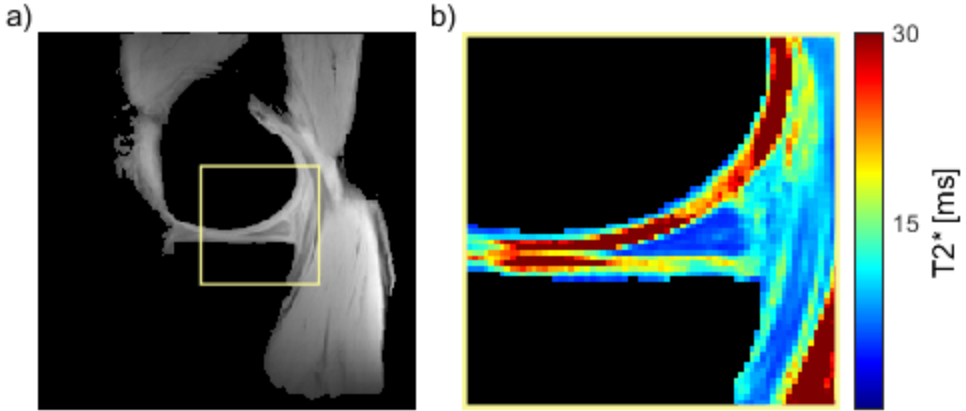


Figure 18 a) Example sagittal UTE image of the medial side of the knee of a healthy volunteer and b) a corresponding T2* map in an area around the meniscus posterior horn (indicated by the yellow square in a). Bone, fat, and air, where the signal is very low, have been masked away

9.2 gagCEST in human articular cartilage

gagCEST has been reported as a promising tool for evaluation of cartilage quality *in vivo*. Validation of the method has commonly been made with phantoms containing CS-A while the GAG in mature human articular cartilage is mainly CS-C. We have reported that the gagCEST effect from CS-C in phantoms is negligible compared to CS-A which raises concerns about what gagCEST reflects in cartilage tissue.

To confirm our findings also in intact cartilage tissue it would be of interest to perform gagCEST measurements in articular cartilage, preferably *in vivo*, and compare to biochemically determined GAG content. Our *ex vivo* experiment, described in chapter 7, was intended for this purpose. However, in this experiment the cartilage layer was very thin and may have already been depleted on GAG since it came from elderly subjects. Future studies should also include healthy tissue as a reference.

It would also be preferable if not only total GAG concentrations could be determined but also specific concentrations of CS-A and CS-C. Disaccharide analysis using HPLC fluoroscopy can be used to determine the concentration of specific GAG types but may be unpractical in the larger number of samples that would be needed for a conclusive result. Also, impurities of the samples might be a problem as purification procedures of small human samples may be difficult.

It would also be of interest to see if the gagCEST method may be specifically adapted to better fit the conditions in the target tissue. So far, optimization has

primarily been based on CS-A and there is a chance that the results are not directly translatable to CS-C. If we want to use gagCEST in adult human articular cartilage it is important that the gagCEST sequence and saturation scheme is adjusted and optimized to fit the specific GAG composition expected in this tissue.

9.3 Meniscus biomechanics

The main function of the meniscus is to distribute load and reduce the pressure on the articular cartilage. This ability originates from the biomechanical properties of the meniscus that comes from the collagen fibre structure, and therefore it is of great interest to study the collagen fibres during loading.

SR-based phase contrast enhanced μ CT offers the possibility of high-resolution 3D imaging of meniscus tissue without the use of tissue fixation or embedding (**Paper IV**). A tissue loading device, e.g., as the one used in the MRI experiment by Nebelung et al. (Nebelung, Dötsch et al. 2020), could potentially be incorporated in the imaging set-up at the synchrotron beamline to image meniscus tissue samples during different loading conditions. The advantage of using this technique is the possibility to directly visualize the collagen fibres, their crimping pattern and how they are affected by tissue loading. To evaluate the images, quantitative parameters relating to tissue degeneration and tissue biomechanics then also needs to be further developed and established.

This could give us new important knowledge of how the meniscus tissue respond to loading in a setting that is more relevant to the *in vivo* case compared to earlier studies using microscopy techniques. To study the biomechanical functions in relation to meniscus degeneration could help shed some light on what happens in the meniscus during development of OA.

10 Acknowledgements

Time flies. I feel as I have just started this project and that there is so much more I would like to do in this research field, I have just scratched the surface. But now is the time to summarize and, slightly surprised, I conclude that it resulted in a thesis in the end. It is only my name written on the front page of the book, but I have not done this work on my own.

First of all, I would like to thank my main supervisor Jonas Svensson who always has good advice when I need it. Secondly, thanks to co-supervisor Pernilla Peterson who always has an idea for a solution or a new experiment. Thank you both for your endless support and positive spirit. Thanks for always taking the time to discuss with me even the smallest of matters.

A big thanks also to co-supervisor Martin Englund for starting up this project, and to everyone at the Clinical Epidemiology Unit for letting me be a part of your group. Thanks also to co-supervisor Patrik Önnérffjord and to everyone at BMC C12 for making me feel welcome in your lab.

To all co-authors of the papers in this thesis: It has been a pleasure to work with all of you!

Thanks also to everyone in the MR physics group in Lund, for letting me be a member of your group. Special thanks to Emelie Lind who showed me how fun it is to do research during my master project. A special thanks also to the people working at the 7T facility and at the 9.4 T scanner at LBIC. Thanks for all the help with measurements and for the company during scanning.

Of course, I also want to thank all of my current and previous colleagues at the department of Medical Radiation Physics in Malmö. Even though I spend a lot of my time in Lund, the department in Malmö always feel like home.

I would also like to express my gratitude to my family: My parents, Jan and Kristina, thanks for always being there when I ask for your help. My sister Sara for all the good talks on our walks. And to my sister Ida who ever since we were little encouraged my curiosity for science. Last, but not least, my dearest Emil and little Tage, thanks for sharing every day with me, I love you both infinitely.

Thanks Everyone, this thesis would not exist without you.
You're the best!

11 List of abbreviations

CS	chondroitin sulphate
CEST	chemical exchange saturation transfer
CT	computed tomography
dGEMRIC	delayed gadolinium enhanced MRI of cartilage
GAG	glycosaminoglycan
gagCEST	glycosaminoglycan chemical exchange saturation transfer
GRE	gradient recalled echo
HPLC	high performance liquid chromatography
IR	inversion recovery
MR	magnetic resonance
MRI	magnetic resonance imaging
μ CT	micro computed tomography
OA	osteoarthritis
SAR	specific absorption rate
SE	spin echo
SR	synchrotron radiation
TE	echo time
TI	inversion time
TKR	total knee joint replacement
TR	repetition time
UTE	ultrashort echo time
WASSR	water saturation shift referencing
QSM	quantitative susceptibility mapping

12 References

- Adams, M. E., M. E. Billingham and H. Muir (1983). "The glycosaminoglycans in menisci in experimental and natural osteoarthritis." Arthritis Rheum **26**(1): 69-76.
- Aspden, R. M., Y. E. Yarker and D. W. Hukins (1985). "Collagen orientations in the meniscus of the knee joint." J Anat **140 (Pt 3)**(Pt 3): 371-380.
- Bae, W. C., J. Du, G. M. Bydder and C. B. Chung (2010). "Conventional and ultrashort time-to-echo magnetic resonance imaging of articular cartilage, meniscus, and intervertebral disk." Top Magn Reson Imaging **21**(5): 275-289.
- Baker-LePain, J. C. and N. E. Lane (2012). "Role of bone architecture and anatomy in osteoarthritis." Bone **51**(2): 197-203.
- Barenius, B., S. Ponzer, A. Shalabi, R. Bujak, L. Norlén and K. Eriksson (2014). "Increased risk of osteoarthritis after anterior cruciate ligament reconstruction: a 14-year follow-up study of a randomized controlled trial." Am J Sports Med **42**(5): 1049-1057.
- Bashir, A., M. L. Gray and D. Burstein (1996). "Gd-DTPA2- as a measure of cartilage degradation." Magn Reson Med **36**(5): 665-673.
- Bayliss, M. T., D. Osborne, S. Woodhouse and C. Davidson (1999). "Sulfation of chondroitin sulfate in human articular cartilage. The effect of age, topographical position, and zone of cartilage on tissue composition." J Biol Chem **274**(22): 15892-15900.
- Berberat, J. E., M. J. Nissi, J. S. Jurvelin and M. T. Nieminen (2009). "Assessment of interstitial water content of articular cartilage with T1 relaxation." Magn Reson Imaging **27**(5): 727-732.
- Betz, O., U. Wegst, D. Weide, M. Heethoff, L. Helfen, W. K. Lee and P. Cloetens (2007). "Imaging applications of synchrotron X-ray phase-contrast microtomography in biological morphology and biomaterials science. I. General aspects of the technique and its advantages in the analysis of millimetre-sized arthropod structure." J Microsc **227**(Pt 1): 51-71.
- Björnsson, S. (1993). "Simultaneous preparation and quantitation of proteoglycans by precipitation with alcian blue." Anal Biochem **210**(2): 282-291.
- Brinkhof, S., R. Nizak, V. Khlebnikov, J. J. Prompers, D. W. J. Klomp and D. B. F. Saris (2018). "Detection of early cartilage damage: feasibility and potential of gagCEST imaging at 7T." Eur Radiol **28**(7): 2874-2881.
- Brinkhof, S., R. Nizak, S. Sim, V. Khlebnikov, E. Quenneville, M. Garon, D. W. J. Klomp and D. Saris (2021). "In vivo biochemical assessment of cartilage with gagCEST MRI: Correlation with cartilage properties." NMR Biomed **34**(3): e4463.

Brown, R. W., Y.-C. N. Cheng, E. M. Haacke, M. R. Thompson and R. Venkatesan (2014). Magnetic resonance imaging: physical principles and sequence design, John Wiley & Sons.

Calixto, N. E., D. Kumar, K. Subburaj, J. Singh, J. Schooler, L. Nardo, X. Li, R. B. Souza, T. M. Link and S. Majumdar (2016). "Zonal differences in meniscus MR relaxation times in response to in vivo static loading in knee osteoarthritis." J Orthop Res **34**(2): 249-261.

Cheung, H. S. (1987). "Distribution of type I, II, III and V in the pepsin solubilized collagens in bovine menisci." Connect Tissue Res **16**(4): 343-356.

Crema, M. D., F. W. Roemer, M. D. Marra, D. Burstein, G. E. Gold, F. Eckstein, T. Baum, T. J. Mosher, J. A. Carrino and A. Guermazi (2011). "Articular cartilage in the knee: current MR imaging techniques and applications in clinical practice and research." Radiographics **31**(1): 37-61.

Diamant, J., A. Keller, E. Baer, M. Litt and R. G. Arridge (1972). "Collagen; ultrastructure and its relation to mechanical properties as a function of ageing." Proc R Soc Lond B Biol Sci **180**(1060): 293-315.

Dube, B., M. A. Bowes, S. R. Kingsbury, E. M. A. Hensor, S. Muzumdar and P. G. Conaghan (2018). "Where does meniscal damage progress most rapidly? An analysis using three-dimensional shape models on data from the Osteoarthritis Initiative." Osteoarthritis Cartilage **26**(1): 62-71.

Dunn, T. C., Y. Lu, H. Jin, M. D. Ries and S. Majumdar (2004). "T2 relaxation time of cartilage at MR imaging: comparison with severity of knee osteoarthritis." Radiology **232**(2): 592-598.

Eijgenraam, S. M., F. A. T. Bovendeert, J. Verschueren, J. van Tiel, Y. M. Bastiaansen-Jenniskens, M. A. Wesdorp, K. Nasserinejad, D. E. Meuffels, J. Guenoun, S. Klein, M. Reijman and E. H. G. Oei (2019). "T2 mapping of the meniscus is a biomarker for early osteoarthritis." Eur Radiol **29**(10): 5664-5672.

Englund, M., A. Guermazi, D. Gale, D. J. Hunter, P. Aliabadi, M. Clancy and D. T. Felson (2008). "Incidental meniscal findings on knee MRI in middle-aged and elderly persons." N Engl J Med **359**(11): 1108-1115.

Englund, M., A. Guermazi, F. W. Roemer, P. Aliabadi, M. Yang, C. E. Lewis, J. Torner, M. C. Nevitt, B. Sack and D. T. Felson (2009). "Meniscal tear in knees without surgery and the development of radiographic osteoarthritis among middle-aged and elderly persons: The Multicenter Osteoarthritis Study." Arthritis Rheum **60**(3): 831-839.

Evans, J. T., R. W. Walker, J. P. Evans, A. W. Blom, A. Sayers and M. R. Whitehouse (2019). "How long does a knee replacement last? A systematic review and meta-analysis of case series and national registry reports with more than 15 years of follow-up." Lancet **393**(10172): 655-663.

Felson, D. T., J. Niu, T. Neogi, J. Goggins, M. C. Nevitt, F. Roemer, J. Torner, C. E. Lewis and A. Guermazi (2016). "Synovitis and the risk of knee osteoarthritis: the MOST Study." Osteoarthritis Cartilage **24**(3): 458-464.

Fernandes, G. S. and A. M. Valdes (2015). "Cardiovascular disease and osteoarthritis: common pathways and patient outcomes." Eur J Clin Invest **45**(4): 405-414.

Folkesson, E., A. Turkiewicz, M. Rydén, H. V. Hughes, N. Ali, J. Tjörnstrand, P. Önnérfford and M. Englund (2020). "Proteomic characterization of the normal human medial meniscus body using data-independent acquisition mass spectrometry." J Orthop Res **38**(8): 1735-1745.

Fox, A. J., F. Wanivenhaus, A. J. Burge, R. F. Warren and S. A. Rodeo (2015). "The human meniscus: a review of anatomy, function, injury, and advances in treatment." Clin Anat **28**(2): 269-287.

Fox, S. A. J., A. Bedi and S. A. Rodeo (2009). "The basic science of articular cartilage: structure, composition, and function." Sports Health **1**(6): 461-468.

Fram, E. K., R. J. Herfkens, G. A. Johnson, G. H. Glover, J. P. Karis, A. Shimakawa, T. G. Perkins and N. J. Pelc (1987). "Rapid calculation of T1 using variable flip angle gradient refocused imaging." Magn Reson Imaging **5**(3): 201-208.

Gelber, P. E., G. Gonzalez, J. L. Lloreta, F. Reina, E. Caceres and J. C. Monllau (2008). "Freezing causes changes in the meniscus collagen net: a new ultrastructural meniscus disarray scale." Knee Surg Sports Traumatol Arthrosc **16**(4): 353-359.

Gong, J., V. Pedoia, L. Facchetti, T. M. Link, C. B. Ma and X. Li (2016). "Bone marrow edema-like lesions (BMELs) are associated with higher T1 ρ and T(2) values of cartilage in anterior cruciate ligament (ACL)-reconstructed knees: a longitudinal study." Quant Imaging Med Surg **6**(6): 661-670.

Gowland, P. and P. Mansfield (1993). "Accurate measurement of T1 in vivo in less than 3 seconds using echo-planar imaging." Magnetic resonance in medicine **30**(3): 351-354.

Guivel-Scharen, V., T. Sinnwell, S. D. Wolff and R. S. Balaban (1998). "Detection of proton chemical exchange between metabolites and water in biological tissues." J Magn Reson **133**(1): 36-45.

Gulani, V., F. Calamante, F. G. Shellock, E. Kanal and S. B. Reeder (2017). "Gadolinium deposition in the brain: summary of evidence and recommendations." Lancet Neurol **16**(7): 564-570.

Hada, S., M. Ishijima, H. Kaneko, M. Kinoshita, L. Liu, R. Sadatsuki, I. Futami, A. Yusup, T. Takamura, H. Arita, J. Shiozawa, T. Aoki, Y. Takazawa, H. Ikeda, S. Aoki, H. Kurosawa, Y. Okada and K. Kaneko (2017). "Association of medial meniscal extrusion with medial tibial osteophyte distance detected by T2 mapping MRI in patients with early-stage knee osteoarthritis." Arthritis Res Ther **19**(1): 201.

Hager, B., S. M. Walzer, X. Deligianni, O. Bieri, A. Berg, M. M. Schreiner, M. Zalaudek, R. Windhager, S. Trattnig and V. Juras (2019). "Orientation dependence and decay characteristics of T2 * relaxation in the human meniscus studied with 7 Tesla MR microscopy and compared to histology." Magn Reson Med **81**(2): 921-933.

Haneder, S., S. R. Apprich, B. Schmitt, H. J. Michaely, S. O. Schoenberg, K. M. Friedrich and S. Trattnig (2013). "Assessment of glycosaminoglycan content in intervertebral discs using chemical exchange saturation transfer at 3.0 Tesla: preliminary results in patients with low-back pain." Eur Radiol **23**(3): 861-868.

Herwig, J., E. Egner and E. Buddecke (1984). "Chemical changes of human knee joint menisci in various stages of degeneration." Ann Rheum Dis **43**(4): 635-640.

Jerosch, J., W. H. Castro and J. Assheuer (1996). "Age-related magnetic resonance imaging morphology of the menisci in asymptomatic individuals." Arch Orthop Trauma Surg **115**(3-4): 199-202.

Jung, K. A., S. C. Lee, S. H. Hwang, K. H. Yang, D. H. Kim, J. H. Sohn, S. J. Song and D. J. Hunter (2010). "High frequency of meniscal hypertrophy in persons with advanced varus knee osteoarthritis." Rheumatol Int **30**(10): 1325-1333.

Juras, V., S. Apprich, S. Zbyn, L. Zak, X. Deligianni, P. Szomolanyi, O. Bieri and S. Trattnig (2014). "Quantitative MRI analysis of menisci using biexponential T2* fitting with a variable echo time sequence." Magn Reson Med **71**(3): 1015-1023.

Kestilä, I., E. Folkesson, M. A. Finnilä, A. Turkiewicz, P. Önnérfford, V. Hughes, J. Tjörnstrand, M. Englund and S. Saarakkala (2019). "Three-dimensional microstructure of human meniscus posterior horn in health and osteoarthritis." Osteoarthritis Cartilage.

Kestilä, I., J. Thevenot, M. A. Finnilä, S. S. Karhula, I. Hadjab, S. Kauppinen, M. Garon, E. Quenneville, M. Haapea, L. Rieppo, K. P. Pritzker, M. D. Buschmann, H. J. Nieminen and S. Saarakkala (2018). "In vitro method for 3D morphometry of human articular cartilage chondrons based on micro-computed tomography." Osteoarthritis Cartilage **26**(8): 1118-1126.

Kim, M., Q. Chan, M. P. Anthony, K. M. Cheung, D. Samartzis and P. L. Khong (2011). "Assessment of glycosaminoglycan distribution in human lumbar intervertebral discs using chemical exchange saturation transfer at 3 T: feasibility and initial experience." NMR Biomed **24**(9): 1137-1144.

Kim, M., J. Gillen, B. A. Landman, J. Zhou and P. C. van Zijl (2009). "Water saturation shift referencing (WASSR) for chemical exchange saturation transfer (CEST) experiments." Magn Reson Med **61**(6): 1441-1450.

Kimelman, T., A. Vu, P. Storey, C. McKenzie, D. Burstein and P. Prasad (2006). "Three-dimensional T1 mapping for dGEMRIC at 3.0 T using the Look Locker method." Invest Radiol **41**(2): 198-203.

Kirsch, S., M. Kreinest, G. Reisig, M. L. Schwarz, P. Strobel and L. R. Schad (2013). "In vitro mapping of 1H ultrashort T2* and T2 of porcine menisci." NMR Biomed **26**(9): 1167-1175.

Kogan, F., B. A. Hargreaves and G. E. Gold (2017). "Volumetric multislice gagCEST imaging of articular cartilage: Optimization and comparison with T1rho." Magn Reson Med **77**(3): 1134-1141.

Krause, M., J. M. Hausherr, B. Burgeth, C. Herrmann and W. Krenkel (2010). "Determination of the fibre orientation in composites using the structure tensor and local X-ray transform." Journal of Materials Science **45**(4): 888-896.

Krishnamoorthy, G., R. P. R. Nanga, P. Bagga, H. Hariharan and R. Reddy (2017). "High quality three-dimensional gagCEST imaging of in vivo human knee cartilage at 7 Tesla." Magn Reson Med **77**(5): 1866-1873.

Krusche-Mandl, I., B. Schmitt, L. Zak, S. Apprich, S. Aldrian, V. Juras, K. M. Friedrich, S. Marlovits, M. Weber and S. Trattnig (2012). "Long-term results 8 years after autologous osteochondral transplantation: 7 T gagCEST and sodium magnetic resonance imaging with morphological and clinical correlation." Osteoarthritis Cartilage **20**(5): 357-363.

Kumm, J., F. W. Roemer, A. Guermazi, A. Turkiewicz and M. Englund (2016). "Natural History of Intrameniscal Signal Intensity on Knee MR Images: Six Years of Data from the Osteoarthritis Initiative." Radiology **278**(1): 164-171.

Kurkijärvi, J. E., M. J. Nissi, I. Kiviranta, J. S. Jurvelin and M. T. Nieminen (2004). "Delayed gadolinium-enhanced MRI of cartilage (dGEMRIC) and T2 characteristics of human knee articular cartilage: topographical variation and relationships to mechanical properties." Magn Reson Med **52**(1): 41-46.

Lee, Y. H., J. Yang, H. K. Jeong and J. S. Suh (2017). "Assessment of the patellofemoral cartilage: Correlation of knee pain score with magnetic resonance cartilage grading and magnetization transfer ratio asymmetry of glycosaminoglycan chemical exchange saturation transfer." Magn Reson Imaging **35**: 61-68.

Ling, W., R. R. Regatte, G. Navon and A. Jerschow (2008). "Assessment of glycosaminoglycan concentration in vivo by chemical exchange-dependent saturation transfer (gagCEST)." Proc Natl Acad Sci U S A **105**(7): 2266-2270.

Liu, F., A. Samsonov, J. J. Wilson, D. G. Blankenbaker, W. F. Block and R. Kijowski (2015). "Rapid in vivo multicomponent T2 mapping of human knee menisci." J Magn Reson Imaging **42**(5): 1321-1328.

Lohmander, L. S., P. M. Englund, L. L. Dahl and E. M. Roos (2007). "The long-term consequence of anterior cruciate ligament and meniscus injuries: osteoarthritis." Am J Sports Med **35**(10): 1756-1769.

Look, D. C. and D. R. Locker (1970). "Time saving in measurement of NMR and EPR relaxation times." Review of Scientific Instruments **41**(2): 250-251.

Martel-Pelletier, J., C. Boileau, J. P. Pelletier and P. J. Roughley (2008). "Cartilage in normal and osteoarthritis conditions." Best Pract Res Clin Rheumatol **22**(2): 351-384.

Melkus, G., M. Grabau, D. C. Karampinos and S. Majumdar (2014). "Ex vivo porcine model to measure pH dependence of chemical exchange saturation transfer effect of glycosaminoglycan in the intervertebral disc." Magn Reson Med **71**(5): 1743-1749.

Menezes, N. M., M. L. Gray, J. R. Hartke and D. Burstein (2004). "T2 and T1rho MRI in articular cartilage systems." Magn Reson Med **51**(3): 503-509.

Michalek, A. J., L. Kuxhaus, D. Jaremczuk and N. L. Zaino (2018). "Proteoglycans contribute locally to swelling, but globally to compressive mechanics, in intact cervine medial meniscus." J Biomech **74**: 86-91.

Mosher, T. J., H. Smith, B. J. Dardzinski, V. J. Schmithorst and M. B. Smith (2001). "MR imaging and T2 mapping of femoral cartilage: in vivo determination of the magic angle effect." AJR Am J Roentgenol **177**(3): 665-669.

Mulat, C., M. Donias, P. Baylou, G. Vignoles and C. Germain (2008). "Axis detection of cylindrical objects in three-dimensional images." Journal of Electronic Imaging **17**(3): 031108.

Müller-Lutz, A., C. Schleich, B. Schmitt, G. Antoch, F. Matuschke, M. Quentin, H. J. Wittsack and F. Miese (2016). "Gender, BMI and T2 dependencies of glycosaminoglycan chemical exchange saturation transfer in intervertebral discs." Magn Reson Imaging **34**(3): 271-275.

Nebelung, S., L. Dötsch, D. Shah, D. B. Abrar, K. Linka, M. Knobe, P. Sewerin, J. Thüning, C. Kuhl and D. Truhn (2020). "Functional MRI Mapping of Human Meniscus Functionality and its Relation to Degeneration." Sci Rep **10**(1): 2499.

Nebelung, S., M. Tingart, T. Pufe, C. Kuhl, H. Jahr and D. Truhn (2016). "Ex vivo quantitative multiparametric MRI mapping of human meniscus degeneration." Skeletal Radiol **45**(12): 1649-1660.

Nelson, A. E. (2018). "Osteoarthritis year in review 2017: clinical." Osteoarthritis Cartilage **26**(3): 319-325.

Nykänen, O., L. Rieppo, J. Töyräs, V. Kolehmainen, S. Saarakkala, K. Shmueli and M. J. Nissi (2018). "Quantitative susceptibility mapping of articular cartilage: Ex vivo findings at multiple orientations and following different degradation treatments." Magn Reson Med **80**(6): 2702-2716.

Nykänen, O., J. K. Sarin, J. H. Ketola, H. Leskinen, N. C. R. Te Moller, V. Tiitu, I. A. D. Mancini, J. Visser, H. Brommer, P. R. van Weeren, J. Malda, J. Töyräs and M. J. Nissi (2019). "T2* and quantitative susceptibility mapping in an equine model of post-traumatic osteoarthritis: assessment of mechanical and structural properties of articular cartilage." Osteoarthritis Cartilage **27**(10): 1481-1490.

Paganin, D., S. C. Mayo, T. E. Gureyev, P. R. Miller and S. W. Wilkins (2002). "Simultaneous phase and amplitude extraction from a single defocused image of a homogeneous object." J Microsc **206**(Pt 1): 33-40.

Pauli, C., S. P. Grogan, S. Patil, S. Otsuki, A. Hasegawa, J. Koziol, M. K. Lotz and D. D. D'Lima (2011). "Macroscopic and histopathologic analysis of human knee menisci in aging and osteoarthritis." Osteoarthritis Cartilage **19**(9): 1132-1141.

Petersen, W. and B. Tillmann (1998). "Collagenous fibril texture of the human knee joint menisci." Anat Embryol (Berl) **197**(4): 317-324.

Peterson, P., E. Olsson and J. Svensson (2019). "T(2) relaxation time bias in gagCEST at 3T and 7T: comparison of saturation schemes." Magn Reson Med **81**(2): 1044-1051.

Pierantoni, M., I. Silva Barreto, M. Hammerman, L. Verhoeven, E. Törnquist, V. Novak, R. Mokso, P. Eliasson and H. Isaksson (2021). "A quality optimization approach to image Achilles tendon microstructure by phase-contrast enhanced synchrotron micro-tomography." Sci Rep **11**(1): 17313.

Poehling, G. G., D. S. Ruch and S. J. Chabon (1990). "The landscape of meniscal injuries." Clin Sports Med **9**(3): 539-549.

Pomin, V. H. (2014). "NMR chemical shifts in structural biology of glycosaminoglycans." Anal Chem **86**(1): 65-94.

Poole, A. R. (2012). "Osteoarthritis as a whole joint disease." Hss j **8**(1): 4-6.

Rauscher, I., R. Stahl, J. Cheng, X. Li, M. B. Huber, A. Luke, S. Majumdar and T. M. Link (2008). "Meniscal measurements of T1rho and T2 at MR imaging in healthy subjects and patients with osteoarthritis." Radiology **249**(2): 591-600.

Rehnitz, C., J. Kupfer, N. A. Streich, I. Burkholder, B. Schmitt, L. Lauer, H. U. Kauczor and M. A. Weber (2014). "Comparison of biochemical cartilage imaging techniques at 3 T MRI." Osteoarthritis Cartilage **22**(10): 1732-1742.

Saar, G., B. Zhang, W. Ling, R. R. Regatte, G. Navon and A. Jerschow (2012). "Assessment of glycosaminoglycan concentration changes in the intervertebral disc via chemical exchange saturation transfer." NMR Biomed **25**(2): 255-261.

Saito, S., Y. Mori, N. Tanki, Y. Yoshioka and K. Murase (2015). "Factors affecting the chemical exchange saturation transfer of Creatine as assessed by 11.7 T MRI." Radiol Phys Technol **8**(1): 146-152.

Schleich, C., A. Müller-Lutz, M. Eichner, B. Schmitt, F. Matuschke, B. Bittersohl, C. Zilkens, H. J. Wittsack, G. Antoch and F. Miese (2016). "Glycosaminoglycan Chemical Exchange Saturation Transfer of Lumbar Intervertebral Discs in Healthy Volunteers." Spine (Phila Pa 1976) **41**(2): 146-152.

Schleich, C., A. Müller-Lutz, L. Zimmermann, J. Boos, B. Schmitt, H. J. Wittsack, G. Antoch and F. Miese (2016). "Biochemical imaging of cervical intervertebral discs with glycosaminoglycan chemical exchange saturation transfer magnetic resonance imaging: feasibility and initial results." Skeletal Radiol **45**(1): 79-85.

Schmitt, B., S. Zbýn, D. Stelzeneder, V. Jellus, D. Paul, L. Lauer, P. Bachert and S. Trattnig (2011). "Cartilage quality assessment by using glycosaminoglycan chemical exchange saturation transfer and (23)Na MR imaging at 7 T." Radiology **260**(1): 257-264.

Schreiner, M. M., Š. Zbýň, B. Schmitt, M. Weber, S. Domayer, R. Windhager, S. Trattnig and V. Mlynárik (2016). "Reproducibility and regional variations of an improved gagCEST protocol for the in vivo evaluation of knee cartilage at 7 T." Magma **29**(3): 513-521.

Singh, A., M. Haris, K. Cai, V. B. Kassey, F. Kogan, D. Reddy, H. Hariharan and R. Reddy (2012). "Chemical exchange saturation transfer magnetic resonance imaging of human knee cartilage at 3 T and 7 T." Magn Reson Med **68**(2): 588-594.

Singh, A., M. Haris, K. Cai, F. Kogan, H. Hariharan and R. Reddy (2014). "High resolution T1ρ mapping of in vivo human knee cartilage at 7T." PLoS One **9**(5): e97486.

Smith, H. E., T. J. Mosher, B. J. Dardzinski, B. G. Collins, C. M. Collins, Q. X. Yang, V. J. Schmithorst and M. B. Smith (2001). "Spatial variation in cartilage T2 of the knee." J Magn Reson Imaging **14**(1): 50-55.

Son, M., S. B. Goodman, W. Chen, B. A. Hargreaves, G. E. Gold and M. E. Levenston (2013). "Regional variation in T1ρ and T2 times in osteoarthritic human menisci: correlation with mechanical properties and matrix composition." Osteoarthritis Cartilage **21**(6): 796-805.

Speer, D. P. and L. Dahners (1979). "The collagenous architecture of articular cartilage. Correlation of scanning electron microscopy and polarized light microscopy observations." Clin Orthop Relat Res(139): 267-275.

Sun, Y., D. R. Mauerhan, J. S. Kneisl, H. James Norton, N. Zinchenko, J. Ingram, E. N. Hanley, Jr. and H. E. Gruber (2012). "Histological examination of collagen and proteoglycan changes in osteoarthritic menisci." Open Rheumatol J **6**: 24-32.

Tiderius, C. J., L. E. Olsson, P. Leander, O. Ekberg and L. Dahlberg (2003). "Delayed gadolinium-enhanced MRI of cartilage (dGEMRIC) in early knee osteoarthritis." Magn Reson Med **49**(3): 488-492.

Togao, O., A. Hiwatashi, T. Wada, K. Yamashita, K. Kikuchi, C. Tokunaga, J. Keupp, M. Yoneyama and H. Honda (2018). "A Qualitative and Quantitative Correlation Study of Lumbar Intervertebral Disc Degeneration Using Glycosaminoglycan Chemical Exchange Saturation Transfer, Pfirrmann Grade, and T1-ρ." AJNR Am J Neuroradiol **39**(7): 1369-1375.

Trattinig, S., V. Mlynárik, M. Breitenseher, M. Huber, A. Zembsch, T. Rand and H. Imhof (1999). "MRI visualization of proteoglycan depletion in articular cartilage via intravenous administration of Gd-DTPA." Magn Reson Imaging **17**(4): 577-583.

van Zijl, P. C., C. K. Jones, J. Ren, C. R. Malloy and A. D. Sherry (2007). "MRI detection of glycogen in vivo by using chemical exchange saturation transfer imaging (glycoCEST)." Proc Natl Acad Sci U S A **104**(11): 4359-4364.

Villegas, D. F. and T. L. Donahue (2010). "Collagen morphology in human meniscal attachments: a SEM study." Connect Tissue Res **51**(5): 327-336.

Volpi, N., F. Galeotti, B. Yang and R. J. Linhardt (2014). "Analysis of glycosaminoglycan-derived, precolumn, 2-aminoacridone-labeled disaccharides with LC-fluorescence and LC-MS detection." Nat Protoc **9**(3): 541-558.

Wada, T., O. Togao, C. Tokunaga, R. Funatsu, Y. Yamashita, K. Kobayashi, Y. Nakamura and H. Honda (2017). "Glycosaminoglycan chemical exchange saturation transfer in human lumbar intervertebral discs: Effect of saturation pulse and relationship with low back pain." J Magn Reson Imaging **45**(3): 863-871.

Wang, H., J. Bai, B. He, X. Hu and D. Liu (2016). "Osteoarthritis and the risk of cardiovascular disease: a meta-analysis of observational studies." Sci Rep **6**: 39672.

Wei, H., R. Dibb, K. Decker, N. Wang, Y. Zhang, X. Zong, W. Lin, D. B. Nissman and C. Liu (2017). "Investigating magnetic susceptibility of human knee joint at 7 Tesla." Magn Reson Med **78**(5): 1933-1943.

Wei, H., E. Gibbs, P. Zhao, N. Wang, G. P. Cofer, Y. Zhang, G. A. Johnson and C. Liu (2017). "Susceptibility tensor imaging and tractography of collagen fibrils in the articular cartilage." Magn Reson Med **78**(5): 1683-1690.

Wei, H., H. Lin, L. Qin, S. Cao, Y. Zhang, N. He, W. Chen, F. Yan and C. Liu (2019). "Quantitative susceptibility mapping of articular cartilage in patients with osteoarthritis at 3T." J Magn Reson Imaging **49**(6): 1665-1675.

Wei, W., B. Lambach, G. Jia, C. Kaeding, D. Flanigan and M. V. Knopp (2017). "A Phase I clinical trial of the knee to assess the correlation of gagCEST MRI, delayed gadolinium-enhanced MRI of cartilage and T2 mapping." Eur J Radiol **90**: 220-224.

Williams, A., Y. Qian, S. Golla and C. R. Chu (2012). "UTE-T2 * mapping detects sub-clinical meniscus injury after anterior cruciate ligament tear." Osteoarthritis Cartilage **20**(6): 486-494.

Wren, T. A. and D. R. Carter (1998). "A microstructural model for the tensile constitutive and failure behavior of soft skeletal connective tissues." J Biomech Eng **120**(1): 55-61.

Zaiss, M., B. Schmitt and P. Bachert (2011). "Quantitative separation of CEST effect from magnetization transfer and spillover effects by Lorentzian-line-fit analysis of z-spectra." J Magn Reson **211**(2): 149-155.

Zhang, M., Y. Li, R. Feng, Z. Wang, W. Wang, N. Zheng, S. Wang, F. Yan, Y. Lu, T. Y. Tsai and H. Wei (2021). "Change in Susceptibility Values in Knee Cartilage

After Marathon Running Measured Using Quantitative Susceptibility Mapping." J Magn Reson Imaging **54**(5): 1585-1593.

Önnerfjord, P., A. Khabut, F. P. Reinholt, O. Svensson and D. Heinegård (2012). "Quantitative proteomic analysis of eight cartilaginous tissues reveals characteristic differences as well as similarities between subgroups." J Biol Chem **287**(23): 18913-18924.

Knee osteoarthritis is a very common condition, but much is still unknown about the early stages of the disease progression. To increase knowledge, research tools are needed which enable studies of joint tissues. In this thesis, imaging-based methods are evaluated for potential use in articular cartilage and meniscus to detect and follow degenerative changes related to osteoarthritis.



Photo: H. V. Hughes

EMMA EINARSSON graduated as a medical physicist from Lund University in 2016. Since then, she has worked with research in the field of MRI, using quantitative imaging techniques for application in osteoarthritis.